The generalized Born model: its foundation, applications, and limitations

Alexey Onufriev*

September 8, 2010

Abstract

The generalized Born (GB) approximation is introduced in the context of the implicit solvent framework. The physical foundations of the model and its derivation from the underlying Poisson-Boltzmann model are presented in detail. Examples of various flavors of the basic GB model are discussed, followed by examples of recent applications of the approximation in molecular modeling and simulations. Several practical issues such as the accuracy/speed trade-offs, and specific computational advantages of GB-based molecular simulations relative to those based on the explicit solvent model are explored. Limitations of the model and future methodological directions and challenges are discussed.

Keywords: Implicit solvent, generalized Born, Poisson-Boltzmann, molecular simulations

*Departments of Computer Science and Physics, 2050 Torgersen Hall, Virginia Tech, Blacksburg, VA 24061

Contents

1 Introduction. The implicit solvent framework.

An accurate description of the solvent environment is essential for realistic biomolecular modeling. Within the *explicit solvent* framework movements of individual water molecules are explicitly calculated. While arguably the most realistic of the current theoretical approaches, this methodology suffers from considerable computational costs, which often becomes prohibitive, especially for molecular systems undergoing significant structural transitions, such as those involved in the folding of proteins. Other problems with the approach include the difficulty, and often inability to calculate relative free energies of molecular conformations; problems arise due to the need to account for the very large number of solvent degrees of freedom.

An alternative that is becoming more and more popular — the *implicit solvent framework*[1–7] — is based on replacing the real water environment consisting of discrete molecules by an infinite continuum with the dielectric and "hydrophobic" properties of water. The implicit solvent framework has several advantages over explicit water representations, especially in molecular dynamics simulations. These include the following.

i) Lower direct computational (CPU) costs for many molecular systems.

ii) Enhanced sampling of conformational space: in contrast to explicit solvent models, solvent viscosity that often slows down conformational transitions can be drastically reduced or even turned off completely within implicit representations.

iii) Effective ways to estimate free energies; since solvent degrees of freedom are taken into account implicitly, estimating free energies of solvated structures is much more straightforward than with explicit water models.

iv) Instantaneous dielectric response from the solvent which eliminates the need for lengthy equilibration of water that is typically necessary in explicit water simulations. This feature of implicit solvent models becomes key when the charge state of the system changes many times during the course of a simulation, as, for example, in constant pH simulations.

v) Implicit averaging over solvent degrees of freedom eliminates the "noise" – an astronomical number of local minima arising from small variations in solvent structure. Energy landscapes of molecular structures are no longer dominated by the noise and start to make sense.

Availability of all of these advantages depends critically on the availability of practical computational mod-

els based on the implicit solvent framework. One such model that has become particularly popular recently is the generalized Born approximation, or simply the "GB". The model provides a relatively simple, computationally robust and effective way to estimate the long-range electrostatic interactions in biomolecular structures – currently the bottle neck for calculations of energy and force estimates in classical all-atom simulations.[8]

The main goal of this article is to introduce the GB model and to present an overview of its current use in molecular modeling. Special emphasis will be given to the discussion of approximations that the model rests upon. The chapter is organized as follows: after a brief introduction into the key approximation of the general implicit solvent framework, I will review the Poisson-Boltzmann model of continuum electrostatics as the foundation of the GB approximation. A derivation of the GB approximation will then be presented, followed by a discussion of the various "flavors" of the model. I will then give examples of some recent uses of the model in molecular modeling. Several issues pertaining to practical aspects of the model will be touched upon in relative detail, including relative computational speed-up and enhancement of conformational sampling that can be achieved via the use of the GB approximation. Limitations of the model will also be discussed, followed by concluding remarks and outlook.

1.1 Key approximations of the implicit solvent framework

In many molecular modeling applications, one needs to compute the total energy of the molecule in the presence of solvent. This energy is a function of molecular configuration, and its gradients with respect to atomic positions determine the forces on the atoms. The total energy of a solvated molecule can be conveniently written as $E_{tot} = E_{vac} + \Delta G_{\rm solv}$, where E_{vac} represents molecule's potential energy in vacuum (gas-phase), and $\Delta G_{\rm solv}$ is defined as the free energy of transferring the molecule from vacuum into solvent, *i.e.* solvation free energy. The above decomposition is already an approximation made by most classical (non-polarizable) force-fields, as it assumes this specific separability of the Hamiltonian. In practice, once the choice of the gas-phase potential function, or force-field, E_{vac} is made, its computation is relatively straightforward.[9] The difficulty comes from the need to estimate the effects of solvent, encapsulated by the $\Delta G_{\rm solv}$ term in the above

equation. At present, one often makes the following simplifying approximation to estimate $\Delta G_{\rm solv}$:

$$\Delta G_{\rm solv} = \Delta G_{\rm el} + \Delta G_{\rm nonpolar}, \tag{1}$$

where $\Delta G_{\rm nonpolar}$ is the free energy of solvating the molecule from which all charges have been removed (i.e. partial charges of every atom are set to zero), and $\Delta G_{\rm el}$ is the free energy of first removing all charges in the vacuum, and then adding them back in the presence of a continuum solvent environment. That Eq. 1 holds only approximately can be seen from the fact that the absolute values of solvation energies of ions of the same size and opposite charge (and the same magnitude) are not identical.[10] It should be noted that Eq. 1 is not an absolutely necessary assumption within the general implicit solvent framework,[11,12] but is the one that most current practical models make. Within this approximation, one needs practical methods of computing both $\Delta G_{\rm el}$ and $\Delta G_{\rm nonpolar}$. Computing the non-polar term has not so far been the computational bottleneck of molecular modeling, perhaps in part due to the simplistic nature of the approximations used to compute it. We will briefly touch upon some of these issues below. Our main focus will be $\Delta G_{\rm el}$ that is presently the most time-consuming part. Accuracy of $\Delta G_{\rm el}$ estimates is of paramount concern since the underlying long-range interactions are critical to function and stability of many classes of biological and chemical structures. To understand the physical basis of *analytical* approximations to $\Delta G_{\rm el}$ such as the GB model, one needs to start with the more fundamental underlying approximation – the Poisson-Boltzmann (PB) model. Below is a brief introduction to the PB theory, geared towards our present goal of deriving the GB approximation from it.

1.2 The Poisson-Boltzmann model

If one accepts the continuum, linear response dielectric approximation for the solvent, then, in the absence of mobile ions, the Poisson equation (PE) of classical electrostatics provides an exact formalism for computing the electrostatic potential $\phi(\mathbf{r})$ produced by an arbitrary charge distribution $\rho(\mathbf{r})$.

$$\nabla[\epsilon(\mathbf{r})\nabla\phi(\vec{r})] = -4\pi\rho(\mathbf{r}). \tag{2}$$

Here, $\epsilon(\mathbf{r})$ represents the position-dependent dielectric constant which equals that of bulk solvent far away from the molecule, and is expected to decrease fairly rapidly across the solute/solvent boundary. For now, we only consider $\rho(\mathbf{r})$ produced by a set of "fixed" atomic charges q_i at positions $\mathbf{r}_i$ inside the dielectric boundary, $\rho_f(\mathbf{r}) = \sum_i q_i \delta(\mathbf{r} - \mathbf{r}_i)$. A common simplification is to assume an abrupt dielectric boundary, that is $\epsilon(\mathbf{r})$ takes only two values: $\epsilon_{\rm in}$ inside the dielectric boundary and $\epsilon_{\rm out}$ outside – the so called "two-dielectric" model. However, even with this assumption, analytical solutions of the PE for arbitrary $\rho(\mathbf{r})$ are available only for a handful of highly symmetric geometries, such as the sphere.[13] At the same time the PE can be solved by a variety of standard numerical methods for essentially any realistic dielectric boundary and arbitrary $\epsilon(\mathbf{r})$. The situation becomes more complicated if one is to consider the effect of mobile ions (salt). Not only will the total charge density on the right-hand side of Eq. 2 depend on the potential, but it will contain non-trivial correlations between ions of finite size which are difficult (though not impossible) to take into account computationally.[14] These correlations may be particularly strong for multi-valent ions. Neglecting all such correlations via a mean-field treatment leads to the Poisson-Boltzmann (PB) equation. Namely, using the Boltzmann distribution for the density of mobile ions inside the potential field $\phi(\mathbf{r})$, we can represent the total charge density as

$$\rho(\mathbf{r}) = \rho_f(\mathbf{r}) + |e| \sum_j n_j z_j exp(-\phi(\mathbf{r})|e|z_j/kT), \tag{3}$$

where n_j and z_j are the bulk density and charge of each ion species j, and $|e|$ is the elementary charge. Substituting $\rho(\mathbf{r})$ from Eq. 3 into the right-hand side of the Poisson yields the full non-linear Poisson-Boltzmann equation, or NLPB. The non-linear nature of the NLPB leads to several unusual properties of $\phi(\mathbf{r})$ derived from it, including the fact that unlike solutions of the PE, the NLPB potential is non-additive: potential due to a collection of charges is not, in general, the sum of individual potentials due to each charge. This property can make some practical calculations, in particular those involved in pK estimates,[15] rather cumbersome. Several more subtle consistency problems exist: a discussion of these issues, including a derivation of the corresponding expression for the electrostatic free energy can be found in Ref. 16. Analytical solutions of the NLPB are not available for arbitrary $\rho_f(\mathbf{r})$, even for a sphere. However, a variety of numerical algorithms for solving the NLPB equation exist, many of them implemented in software packages designed specifically for biomolecular modeling, for example `APBS`[17] or `DELPHI`.[2,18,19] In this very brief discussion we omit the details of these

numerical procedures along with all of the related technical issues that are discussed in detail elsewhere, see *e.g.* Ref. 20 or Ref. 21 which also contains a comprehensive list of the popular software packages that solve the NLPB equation and its more commonly used linearized version in a variety of contexts.

The complexity of the NLPB equation can be drastically reduced, and the familiar properties of the PE restored if the exponential in Eq. 3 is linearized. The corresponding linear Poisson-Boltzmann equation, or simply the PB equation, is commonly used in biomolecular simulations:[22]

$$\nabla[\epsilon(\mathbf{r})\nabla\phi(\vec{r})] = -4\pi\rho_f(\mathbf{r}) + \kappa^2\epsilon(\mathbf{r})\phi(\mathbf{r}). \tag{4}$$

Here the electrostatic screening effects of (monovalent) salt enter via the second term on the right-hand side of Eq.4, where the Debye-Huckel screening parameter $\kappa \approx 0.1[\mathring{A}^{-1}]$ at physiological conditions. Once the potential $\phi(\mathbf{r})$ is computed, the electrostatic part of the solvation free energy is given by the familiar expression of classical electrostatic:

$$\Delta G_{\rm el} = \frac{1}{2}\sum_i q_i[\phi(\mathbf{r}_i) - \phi(\mathbf{r}_i)|_{vac}], \tag{5}$$

where $\phi(\mathbf{r}_i)|_{vac}$ is the electrostatic potential computed for the same charge distribution in the absence of the dielectric boundary, *e.g.* in vacuum. Note that this simple formula is only valid for the linearized PB equation.

2 The generalized Born model

The need for computationally facile approximations for $\Delta G_{\rm el}$ requires further trade-offs between accuracy and speed, especially in dynamical applications where speed and algorithmic simplicity is paramount. One such approximation is the generalized Born (GB) model. The analytical GB method is an approximate, relative to the PB model, way to calculate the electrostatic part of the solvation free energy, $\Delta G_{\rm el}$. The methodology has become particularly popular in molecular dynamics (MD) applications,[23–29] and lately in many other areas that will be discussed below.

2.1 Theoretical foundation of the GB model

We will begin by re-casting the Poisson equation 2 in an equivalent form for the Green function:[30]

$$\nabla[\epsilon(\mathbf{r})\nabla\mathbf{G}(\mathbf{r}_i,\mathbf{r}_j)] = -4\pi\delta(\mathbf{r}_i-\mathbf{r}_j), \tag{6}$$

Within the two-dielectric model, the solution inside the dielectric boundary is

$$\mathbf{G}(\mathbf{r}_i,\mathbf{r}_j) = \frac{1}{\epsilon_{\rm in}|\mathbf{r}_i-\mathbf{r}_j|} + \mathbf{F}(\mathbf{r}_i,\mathbf{r}_j), \tag{7}$$

The first term in the Green function has the familiar form of the Coulomb potential due to a single charge source, while the second term satisfies the Laplace equation $\nabla^2\mathbf{F}(\mathbf{r}_i,\mathbf{r}_j)=0$. Here, $\mathbf{F}(\mathbf{r}_i,\mathbf{r}_j)$ corresponds to the reaction field due to polarization charges induced at the boundary; $\mathbf{F}(\mathbf{r}_i,\mathbf{r}_j)\neq 0$ only in the presence of the boundary. Comparing $\mathbf{G}(\mathbf{r}_i,\mathbf{r}_j)$ with Eq. 5 we see that

$$\Delta G_{\rm el} = \frac{1}{2}\sum_{ij}\mathbf{F}(\mathbf{r}_i,\mathbf{r}_j)q_iq_j \tag{8}$$

Of course, computing $\mathbf{F}(\mathbf{r}_i,\mathbf{r}_j)$ for an arbitrary charge distribution inside an arbitrary molecular boundary is as hard as solving the original Poisson equation, and can only be done numerically as mentioned in the previous section. To make progress towards our goal—finding a simple, closed form formula for $\Delta G_{\rm el}$— we need to make further approximations. We will pursue the following strategy: use a known analytical solution of the PE for some very simple dielectric boundary to get a specific *analytical* form of $\mathbf{F}(\mathbf{r}_i,\mathbf{r}_j)$. Since for biomolecular modeling we need to consider arbitrary distribution of partial charges inside the dielectric boundary, our choice is essentially limited to just one shape: the sphere, for which an exact solution of the PE exists.[13] We follow Ref.[31] and separate the self-contribution, $\mathbf{F}(\mathbf{r}_i,\mathbf{r}_i)$, from the interaction part, $\mathbf{F}(\mathbf{r}_i,\mathbf{r}_j)$:

$$\mathbf{F}(\mathbf{r}_i,\mathbf{r}_i)^{\rm sphere} = -\left(\frac{1}{\epsilon_{\rm in}}-\frac{1}{\epsilon_{\rm out}}\right)\frac{1}{A}\sum_{l=0}^{\infty}\frac{t_{ii}^l}{1+\frac{l}{l+1}\beta} \tag{9}$$

$$\mathbf{F}(\mathbf{r}_i,\mathbf{r}_j)^{\rm sphere} = -\left(\frac{1}{\epsilon_{\rm in}}-\frac{1}{\epsilon_{\rm out}}\right)\frac{1}{A}\sum_{l=0}^{\infty}\frac{t_{ij}^l P_l(\cos\theta)}{1+\frac{l}{l+1}\beta} \tag{10}$$

where $t_{ij} = r_i r_j / A^2$, $r_i = |\mathbf{r}_i|$ is the atom's position relative to the center of the sphere, A is the molecule's radius, θ is the angle between $\mathbf{r}_i$ and $\mathbf{r}_j$, and $\beta = \epsilon_{\rm in}/\epsilon_{\rm out}$ (see Fig. 2).

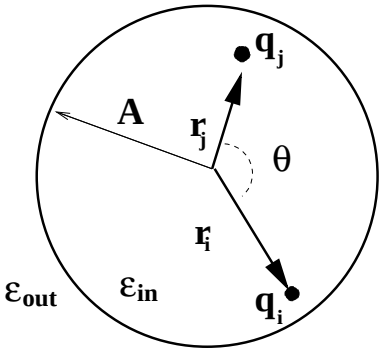

Figure 1:

Figure 2: Illustration for Eqs. 9, 10: a sphere of dielectric $\epsilon_{\rm in}$ and radius A with two charges, q_i and q_j at positions $\mathbf{r}_i$ and $\mathbf{r}_j$ relative to the sphere's center. The sphere is surrounded by infinite medium of uniform dielectric $\epsilon_{\rm out}$.

The expression for $\mathbf{F}(\mathbf{r}_i, \mathbf{r}_j)$, Eq. 10, is extremely valuable because it is *exact*. However, its use in practical computational problems is limited because the corresponding infinite series converges slowly when t_{ij} approaches one.[32] The latter is the typical case for biomolecules where largest charges are likely to be found near molecular surface. However, under certain assumptions the series in Eq. 10 can be summed to produce simple, finite expressions.[31,33] Here is an outline of the derivation. Consider the typical case of aqueous solvation $\epsilon_{\rm out} \gg \epsilon_{\rm in} \geq 1$. After making the approximation $\epsilon_{\rm out} \to \infty$, which in this case is equivalent to $\beta = 0$, the dependence on l in the denominators of the fractions in Eq. 10 disappears, and we can use the well-known identity for the sum of Legendre polynomials[31] along with the geometrical identity $\cos\theta = (r_i^2 + r_j^2 - r_{ij}^2)/2r_i r_j$ (r_{ij} is the distance between the charges) to obtain for $\mathbf{F}(\mathbf{r}_i, \mathbf{r}_j)^{\rm sphere}$:

$$\mathbf{F}(\mathbf{r}_i, \mathbf{r}_i)^{\rm sphere} = -\frac{1}{\epsilon_{\rm in}} \frac{1}{A - r_i^2/A} \tag{11}$$

$$\mathbf{F}(\mathbf{r}_i, \mathbf{r}_j)^{\rm sphere} = -\frac{1}{\epsilon_{\rm in}} \frac{1}{\sqrt{r_{ij}^2 + \left(A - \frac{r_i^2}{A}\right)\left(A - \frac{r_j^2}{A}\right)}} \tag{12}$$

The above equations along with Eq. 8 solve the problem of finding a simple, analytical formula for $\Delta G_{\rm el}$, albeit in the $\epsilon_{\rm out} \to \infty$ limit. However, it is not yet clear what parameters such as A, and especially "distance to center" r_i, Fig. 2, mean in the case of realistic molecular shapes. Fortunately, the specific form of Eqs. 11 and 12 provides a solution that is one of the cornerstones of the GB theory. Note that both the cross-term $\mathbf{F}(\mathbf{r}_i, \mathbf{r}_j)^{\rm sphere}$ and the self-term $\mathbf{F}(\mathbf{r}_i, \mathbf{r}_i)^{\rm sphere}$ of the Green function depend only on $(A - r_i^2/A)$ – the quantity we will call *the effective Born radius* R_i of atom i. Thus, if we are somehow able to compute the self-term $\mathbf{F}(\mathbf{r}_i, \mathbf{r}_i)$, or equivalently $\Delta G_{ii}^{\rm el}$, for every atom in the molecule, then we can invert Eq. 11 to calculate $(A - r_i^2/A)(A - r_j^2/A) = R_i R_j$, insert these into Eq. 12, and hence obtain the cross-terms $\mathbf{F}(\mathbf{r}_i, \mathbf{r}_j)$ as a function of R_i, R_j, and r_{ij}. For realistic biomolecular shapes the specific form of $\mathbf{F}(\mathbf{r}_i, \mathbf{r}_j)$ currently used by the generalized Born is slightly more complicated than $\mathbf{F}(\mathbf{r}_i, \mathbf{r}_j)^{\rm sphere}$ of Eq. 12:

$$R_i = -\frac{1}{2}\left(\frac{1}{\epsilon_{\rm in}} - \frac{1}{\epsilon_{\rm out}}\right)\frac{q_i^2}{\Delta G_{ii}^{\rm el}} \tag{13}$$

$$\Delta G_{\rm el} = \frac{1}{2}\sum_{ij}\mathbf{F}(\mathbf{r}_i, \mathbf{r}_j) q_i q_j \approx -\frac{1}{2}\left(\frac{1}{\epsilon_{\rm in}} - \frac{1}{\epsilon_{\rm out}}\right)\sum_{i,j}\frac{q_i q_j}{\sqrt{r_{ij}^2 + R_i R_j \exp\left(-\gamma \frac{r_{ij}^2}{R_i R_j}\right)}} \tag{14}$$

The above form of $\mathbf{F}(\mathbf{r}_i, \mathbf{r}_j)$ with $\gamma = 1/4$ is due to Still *et al.*[34] and is the most common form of $\mathbf{F}(\mathbf{r}_i, \mathbf{r}_j)$ used in practice today, although alternatives such as $\gamma = 1/2$ or $\gamma = 1/10$ have also been explored. The Still's formulae, which we will refer to as the GB model or "canonical" GB, differ from the exact sphere-based Eqs. 11 in two respects: the use of $\gamma \neq 0$*, and slightly different dependence on the dielectrics via the pre-factor $\left(\frac{1}{\epsilon_{\rm in}} - \frac{1}{\epsilon_{\rm out}}\right)$. Unless the charge is positioned exactly in the sphere's center the specific dependence of Eq. 14 on $\epsilon_{\rm in}, \epsilon_{\rm out}$ is approximate even for a perfect sphere: the corresponding error increases with decreasing $\epsilon_{\rm out}$.[31,35] Ways to improve the approximation are considered in Sec. 2.5. To better understand the effect of non-zero γ, note that setting $\gamma \to 0$ in the Still's formula recovers the sphere limit of Eq. 12; the use of $\gamma \neq 0$ leads to more accurate estimates of $\Delta G_{\rm el}$ for non-spherical geometries of realistic molecules. This is likely due to the fact that, for a non-spherical molecule, many pairs of charges exist for which more of the electric field lines between the charges go through the high dielectric region, effectively reducing the pairwise interaction

*As a result, $\mathbf{F}(\mathbf{r}_i, \mathbf{r}_j)$ from Eq. 14 does not satisfy the Laplace equation.

compared to the purely spherical, everywhere convex molecular boundary. The Still's form of $\mathbf{F}(\mathbf{r}_i, \mathbf{r}_j)$ takes this effect into account, at least to some extent, by allowing for steeper decay of the charge-charge interaction with the distance. To perform practical computations based on Eq. 14 one needs the effective Born radii R_i for every atom. The effective radius represents the atom's degree of burial within the low dielectric solute. By definition, the effective radius can be obtained by computing $\Delta G^{\rm el}_{ii}$ for each atom i, and then inverting Eq. 13.* In fact, Eq. 13 is simply the inverse of the the famous Born formula for the solvation energy of a single ion. The idea of "generalization" of the Born formula to account for solvation energy of small molecules dates back at least 50 years,[36] although the term "generalized Born" did not seem to appear in literature until about 25 years ago.[37] Assuming that effective Born radii can be computed efficiently for every atom in the molecule, computational advantages of Eq. 14 relative to numerical PB treatment become apparent: knowledge of only N self-energy terms $\Delta G^{\rm el}_{ii}$, or equivalently, values of R_i for each of N atoms in the molecule gives, via the GB Eq. 14, a quick *analytical* estimate of the remaining $\sim \frac{1}{2}N^2$ charge-charge interaction contributions to the total electrostatic solvation energy. Not less important is the fact that the GB formula is very simple, its analytical derivatives with respect to atomic positions provide the forces needed in dynamical applications. Two immediate questions arise: (i) how can the effective radii be computed *accurately* and efficiently to fully utilize these advantages? and (ii) even if the R_is are computed very accurately, will the GB formula, Eq. 14, yield reasonably accurate estimates of the electrostatic solvation energies for *realistic molecular shapes*? A positive answer to the second question came from an analysis of the GB accuracy in the case where $\Delta G^{\rm el}_{ii}$ and hence R_is are computed by solving the Poisson equation directly via highly accurate numerical techniques. The resulting sets of R_is—the so-called "perfect radii"—were shown to yield estimates of individual pairwise solvation cross-term energies $\Delta G^{\rm el}_{ij} = q_i q_j \mathbf{F}(\mathbf{r}_i, \mathbf{r}_j)$ in a reasonable agreement with numerical results based on solving the PE directly,[38] Fig. 4.

The PE-based perfect effective radii are very helpful in the analysis and further development of the GB model as they probe the limits of Eq. 14 and provide a natural reference point for approximated effective radii. The perfect radii may also be useful in some practical cases, for example in MD simulations of proteins in their native states, if one assumes that the effective radii can be held constant through the simulation.[38] However, in

*In case of homogeneous solvent of constant dielectric, the correct procedure is to compute the radii in the $\epsilon_{\rm out} \to \infty$ limit, which eliminates the error due to approximate nature of the $\left(\frac{1}{\epsilon_{\rm in}} - \frac{1}{\epsilon_{\rm out}}\right)$ prefactor, see Ref. 31 for details.

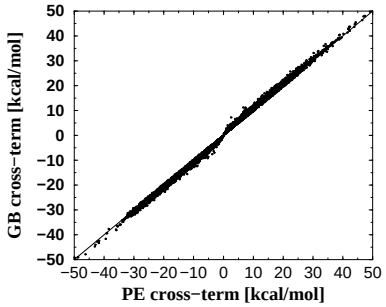

Figure 3:

Figure 4: Comparison of individual cross terms between the perfect-radii GB model (ij terms of Eq. 14) to the corresponding cross terms computed directly from PE equation for the native state of myoglobin. The line $x = y$ represents a perfect match between the GB and PE theories.

most cases the overhead costs of performing a full PE calculation every time the radii need to be computed are prohibitive. Thus, the development of approximate methods for estimation of R_i becomes critical for the GB field. In fact, since all of the current GB models use the same basic equation 14, the differences between the many GB "flavors" currently available mostly reflect the differences between the particular procedures used to compute the effective Born radii. In what follows we will introduce the basic ideas behind these procedures.

2.2 Computing the effective Born radii

In practice, the effective radius for each atom i can be calculated by approximately evaluating the electrostatic part of solvation free energy $\Delta G_{ii}^{\mathrm{el}}$ in Eq. 13 via an appropriate volume integral,[39–45] see below. Equivalent formulations based on surface integrals also exist.[46,47] Two main challenges have to be overcome on the way to developing accurate and facile methods for computing the effective radii: (i) finding a computationally simple, physically justified integral representation for $\Delta G_{ii}^{\mathrm{el}}$, and (ii) developing numerical routines to perform the integration over specific volume/surface corresponding to a physically realistic dielectric boundary between the solute and the solvent.

2.2.1 The integral approaches

The goal is to find an approximation for computing the effective Born radius for a given atom i inside a molecule. Classical electrostatics provides an approach for calculating the work done to create a given charge distribution within the molecule:

$$G = \frac{1}{8\pi} \int_{R^3} \frac{\left[\vec{D}(\vec{r})\right]^2}{\epsilon(\vec{r})} d^3\vec{r} \tag{15}$$

where $\vec{D}(\vec{r})$ is the dielectric displacement vector, and $\epsilon(\vec{r})$ is the position-dependent dielectric constant. Now let's zero out all of the charges inside the molecule except for the one on the atom in question. Consider a process in which this molecule is transferred from a medium of uniform dielectric constant $\epsilon_{\rm in}$ equal to that of the solute into the uniform solvent medium $\epsilon_{\rm out}$. The process creates the dielectric boundary which coinsides with the molecular bondary. Then, the electrostatic part of the solvation free energy $\Delta G_{\rm el}$ of the charge, that is the work of transferring this one charge i from a medium of uniform dielectric constant $\epsilon_{\rm in}$ equal to that of the solute, into the two-dielectric solute/solvent medium is:

$$\begin{aligned} \Delta G_{ii}^{\rm el} \;=\; & \frac{1}{8\pi\epsilon_{\rm out}} \int_{\rm solvent} \left[\vec{D}_i(\vec{r})\right]^2 d^3\vec{r} + \frac{1}{8\pi\epsilon_{\rm in}} \int_{\rm solute} \left[\vec{D}_i(\vec{r})\right]^2 d^3\vec{r} \\ & - \frac{1}{8\pi\epsilon_{\rm in}} \int_{\rm solvent} \left[\vec{D}_i^0(\vec{r})\right]^2 d^3\vec{r} - \frac{1}{8\pi\epsilon_{\rm in}} \int_{\rm solute} \left[\vec{D}_i^0(\vec{r})\right]^2 d^3\vec{r} \end{aligned} \tag{16}$$

where $\vec{D}_i(\vec{r})$ is the total dielectric displacement due to charge i, $\epsilon_{\rm out}$ in the dielectric of the solute, and

$$\vec{D_i^0}(\vec{r}) \equiv \frac{q_i}{r^3}\vec{r}, \tag{17}$$

is the Coulomb field created by point charge q_i in the uniform dielectric environment. The above equation is an exact result that would lead to perfect effective radii if $\vec{D}_i(\vec{r})$ were known. Since for an arbitrary molecular shape it is unknown, one makes approximations to $\vec{D}_i(\vec{r})$ to make progress. The Coulomb field approximation – CFA – is historically the first approximation of that nature. It makes what appears to be a fairly drastic assumption,

$$\vec{D}_i(\vec{r}) \approx \vec{D_i^0}(\vec{r}) \equiv \frac{q_i}{r^3}\vec{r}, \tag{18}$$

that is the electric field generated by the atomic point charge is assumed unaffected by the dielectric boundary. With this assumption, the integrals over the solute volume in Eq. 16 cancel, while the solvent volume integrals combine, to yield just one integral over the region exterior to the molecule:

$$\begin{aligned} \Delta G_{ii}^{\mathrm{el}} &= \frac{1}{8\pi}\Big(\frac{1}{\epsilon_{\mathrm{out}}}-\frac{1}{\epsilon_{\mathrm{in}}}\Big)\int\limits_{\mathrm{ext}}\left[\vec{D}_i^0(\vec{r})\right]^2 d^3\vec{r} \\ &= \Big(\frac{1}{\epsilon_{\mathrm{out}}}-\frac{1}{\epsilon_{\mathrm{in}}}\Big)\frac{{q_i}^2}{8\pi}\int\limits_{\mathrm{ext}}\frac{1}{r^4}d^3\vec{r} \end{aligned} \tag{19}$$

Comparing the above with the definition of effective radius in Eq. 13, we arrive at the following expression for the inverse effective radius in the CFA approximation:

$$\alpha_4 = R_i^{-1} = \frac{1}{4\pi}\int\limits_{ext}\frac{1}{|\mathbf{r}-\mathbf{r}_i|^4}dV = \rho_i^{-1} - \frac{1}{4\pi}\int\limits_{r>\rho_i}|\mathbf{r}|^{-4}dV \tag{20}$$

where in the first expression the integral is taken over the region outside of the molecule. The second formula in the equation above is often used for computational convenience:[42] the origin is moved to the atom of interest, and the integration region is the interior of the molecule outside of the atom's VDW radius ρ_i. Effective ways to compute the integral will be discussed below.

The CFA is exact for a point charge at the center of a perfectly spherical solute, but it overestimates effective radii for realistic molecular geometries[48] as well as for spherical regions when the charge is off center.[33] However, many practical routines available today still use the CFA, with a few notable exceptions discussed below. A fortuitous cancellation of errors[38] enhanced by elaborate parametrizations, plus computational efficiency of the approximation have contributed to its success so far. Still, the limitations of the CFA were known for quite some time, and a search for better approximations to R_i continued. In particular, a class of models exists that approximates the effective radii via integral expressions similar to Eq. 20, but with the integrand different from the CFA's r^{-4}, namely

$$\alpha_N = \left(\frac{1}{4\pi}(N-3)\int\limits_{ext}\frac{dV}{|\mathbf{r}-\mathbf{r}_i|^N}\right)^{\frac{1}{(N-3)}} = \left(\rho_i^{3-N} - \frac{1}{4\pi}(N-3)\int\limits_{r>\rho_i}\frac{dV}{|\mathbf{r}-\mathbf{r}_i|^N}\right)^{\frac{1}{N-3}}, \tag{21}$$

where $N > 3$, and the additional prefactor and exponentiation are needed to preserve the dimension of α_N to be inverse length. Empirical corrections to the CFA based on a simple linear or a rational combination of α_N expressions have lead to significant improvements in accuracy of the GB model.[43,44] Several GB flavors termed "GBMV" based on these approximations have been implemented in CHARMM , such expression involving α_4 and α_5,[48] and later an even more accurate expression—"GBMV2" — based on α_4 and α_7 respectively,[44] $R^{-1} = (1 - \frac{\sqrt{2}}{2})\alpha_4 + \frac{\sqrt{2}}{2}\alpha_7$. While all $N \neq 4$ expressions in Eq. 21 may appear purely heuristic, at least one of them has a rigorous foundation: $N = 6$ yields the *exact* effective radius for any charge inside a perfect spherical boundary,[33] not just at its center as is the case with the CFA. More precisely, the α_6 expression is exact in the $\epsilon_{\rm out} \to \infty$ limit, that is $\Delta G^{\rm el}_{ii} = -\frac{1}{2}\frac{q_i \alpha_6}{\epsilon_{\rm in}}$ Numerical tests show, see Ref. 49 for important details, that if accurately computed "R6" radii are used in the GB equation 14 the resulting electrostatic solvation energies can, on average, be as accurate (relative to the PE reference) as the ones obtained with the use of the perfect radii. An important conclusion made in Ref. 49 was that the following expression based on just one integral

$$\alpha_6 = R_i^{-1} = \left(\frac{3}{4\pi} \int\limits_{ext} \frac{dV}{|\mathbf{r} - \mathbf{r}_i|^6} \right)^{\frac{1}{3}} = \left(\rho_i^{-3} - \frac{3}{4\pi} \int\limits_{r>\rho_i} |\mathbf{r}|^{-\mathbf{6}} dV \right)^{\frac{1}{3}} \tag{22}$$

represents a sufficient solution to the problem of calculating effective radii: further attempts to increase their agreement with PB results would unlikely succeed in improving the accuracy of the GB model itself in its canonical version due to Still, Eq. 14. The above claim makes even more sense if we recall that the "canonical" GB Eq. 14 has the same underlying physical basis as the *R6* approximation for the effective radii: the Kirkwood spherical model. Although the R6 radii can sometimes deviate significantly from the perfect radii, the deviations occur for those geometries where the sphere-based canonical GB, Eq. 14, is itself not expected to work. It remains to be seen whether the potential advantages of Eq. 22 will translate into practical gains once its implementations, which are beginning to appear, will have been extensively tested by the modeling community. Note that in practical GB models, the accuracy of the R6 prescription may be significantly reduced by approximations made by fast routines employed to compute the integral in Eq. 22 or its equivalents. In general, computing the αN integrals over a physically realistic representation of molecular interior (or surface) is a challenge in its own right that we will discuss next.

2.2.2 Representations of the dielectric boundary

Exactly what geometrical object most closely approximates the solute/solvent dielectric boundary is still an unsettled question. Traditionally, PE or PB calculations employed the molecular (Connolly) surface for this purpose,[15] although a boundary with a "smooth" transition between the two dielectrics is coming into use as well.[7,50] The question is even more critical for the development of the GB model than for numerical PB solvers: not only will the precise position of the boundary determine the numerical values of the integrals in Eqs. 20, 21 or 22, and thus the accuracy of the effective Born radii, but the mathematical form of the boundary will also determine how hard it is to find analytical approximations to the integrals.

The two limiting case representations of the dielectric boundary commonly used for the purpose of computing the effective radii are shown in Fig. 5. On the low end of the complexity spectrum, one has the simple and efficient model in which the solute is represented by atomic spheres of the appropriate (VDW) radii for each atom type; the dielectric boundary is taken to coincide with the surface of the spheres. In the other limiting case the dielectric boundary is taken to be coincident with the molecular surface, and thus the integration volume is the intricate molecular volume (MV). Comparisons with explicit solvent calculations show that the latter is a closer approximation to physical reality[51] for macromolecules, but the higher degree of realism comes at a high price: the complexity of molecular volume makes it very hard to approximate the corresponding volume integrals analytically. Practical routines for computing the effective radii often make additional modifications to the two basic volume definitions; for example the sharp dielectric boundaries in both representations can be "smoothed out", *e.g.* via the use of atom-centered Gaussian functions. Existing GB flavors can be further classified by the specific dielectric boundary representations that the flavor is based upon. For example, the integral in Eq. 20 can be computed numerically without further approximations over any reasonable volume representation, including the exact MV.[6] The GB flavors based on such numerical quadratures[6,34,44,46,48,52] are in some sense similar to the "perfect" radii flavor introduced before – they play a significant role in the development of the theory, but their applicability domain is limited, particularly in dynamics where the GB model can be expected to offer most advantages over the PB treatment and explicit solvent.

On the other end of the "volume approximation spectrum" are GB flavors that use the VDW-based dielectric boundary to compute integrals such as Eqs. 20 or 21 in an efficient manner. One such flavor, GBSW[52] available

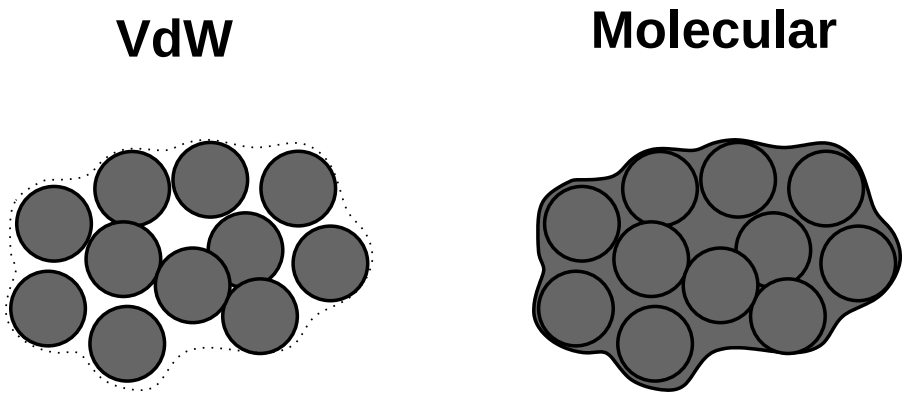

Figure 5: The two limiting cases of computational approximations for the solute–solvent dielectric boundary. In the simpler vdW-based approach (left), the boundary coincides with the surface of atomic spheres, and the interstitial space is treated as high dielectric solvent. The other approximation utilizes molecular surface (MV) for the boundary: all space inside the surface is considered low dielectric solute.

in CHARMM , uses a smooth dielectric boundary based on the VDW volume definition, with the integrand being a rational combination of α_4 and α_7. Recently, VDW-based approximations for the $R6$ GB (based on α_6, Eq. 22) also appeared.[53,54] Another example of the VDW-based approach is one of the first, and still widely used, GB flavor— the HCT model[39,40]— that employs the sharp VDW-based dielectric boundary to compute the CFA integral in Eq. 20 in an efficient manner. Namely, the integral for each atom i is represented as a pairwise sum of integrals over spherical volumes of individual atoms $j \neq i$:

$$\alpha_4 = R_i^{-1} \approx \rho_i^{-1} - \frac{1}{4\pi} \sum_j \int\limits_{|\mathbf{r}_{ij}-\mathbf{r}|<\rho_i} |\mathbf{r}|^{-4} d^3\mathbf{r} \tag{23}$$

The key advantage of the above approximation is that simple analytical expressions are available for it, as well as for the more general case of $\int\limits_{|\mathbf{r}_{ij}-\mathbf{r}|<\rho_i} |\mathbf{r}|^{-N} d^3\mathbf{r}$ for any N, thus providing analytical expressions for α_N in Eq. 21. Variants of the HCT are available in many modeling packages including AMBER[55] and TINKER.[56]

One relatively minor problem with the VDW-based pair-wise approximation such as Eq. 23 is that it neglects possible overlaps between neighboring atoms outside of the atom of interest. In practice, the resulting over-counting of volume can be partially compensated by scaling the intrinsic radii ρ_j by a set of empirically adjusted scaling factors $\rho_j \rightarrow \rho_j * f_j$ where $f_j \leq 1$ typically depend on atom type.

A more serious problem with Eq. 23 based directly on the VDW definition of solvent volume, Fig. 5, is

the neglect of interstitial spaces between the atomic spheres in the interior of the molecule. In other words, these crevices are treated as if they belonged to the solvent space, that is filled with high dielectric. As a result, the effective radii are underestimated. For molecules with little interior the error is small, which probably explains why the original HCT model worked so well for small molecules. Also, the use of CFA leads to a certain cancellation of errors in this case since the CFA tends to overestimate the effective radii. However, for biopolymers, such as proteins or DNA, the neglect of interstitial space leads to appreciable underestimation of the effective radii, compared to the "perfect" radii based on numerical PE estimates that use molecular surface for the dielectric boundary.[38] Efforts to correct this deficiency while preserving the algorithmic simplicity and computational efficiency of the pairwise approximation have led to a series of GB flavors. In one of them, GB^{OBC} (available, for example, in `AMBER` , `NAB` and `TINKER` packages), an empirical correction is introduced[45] that modifies the pairwise integration method, Eq. 23, to reduce the effect of interstitial high dielectrics. The procedure is designed to leave the small radii almost unaffected while larger radii are scaled up, with the scaling factor depending on the magnitude of the radius. The parameters of the re-scaling function were determined based on a training set that included several proteins, both in their folded and unfolded states. Since the VDW-based pair-wise HCT approach is already known to give rather accurate effective radii for surface atoms, but substantially underestimates the larger effective radii for deeply buried atoms, the rescaled radii in GB^{OBC} improve agreement with PB solvation free energies. The computational expense of the rescaling function is minimal so that the efficiency of the HCT method is retained. In addition, effective radii are smoothly capped at about 30 Å , avoiding potential problems with numerical stability. Without the capping, stability problems may arise when the sum of volume integrals in Eq. 23 becomes very close to ${\rho_i}^{-1}$, making the value of the corresponding effective radius very sensitive to tiny structural variations.

However, by design, the GB^{OBC} rescaling function with tabulated parameters compensates for interstitial high dielectric only on average, in a geometry-independent manner. The problem becomes transparent in the limiting case of just two atoms that move relative to each other: while parameters of the re-scaling procedure can in principle be so tabulated as to produce the correct answer for one inter-atomic distance, the method will completely miss changes in molecular volume associated with the relative motion of the atoms. To address this deficiency, an additional correction to the pair-wise procedure was introduced[57] that brings in elements

of molecular volume, in a pair-wise sense. Namely, an additional term is added to Eq. 23 that re-introduces the molecular volume between each pair of atoms missed by the original approximation. The integral over this neck-shaped region can be approximated by a simple analytical function that carries only a small computational overhead relative to GB^{OBC}. At the same time, compared to its predecessors, the resulting GBn flavor, was found to be a noticeably more faithful approximation of electrostatic solvation effects in proteins, not only by comparisons with the PE, but also with explicit solvent MD simulations.[57] The flavor is now also available in `AMBER`,

The "high interstitial dielectric" is not the only problem that needs to be addressed within the pair-wise VDW approach. An approach to better approximate variations in the integration volume associated with changes in molecular geometry—an all-important issue in MD simulations—is presented by AGB and $AGNPB$ flavors[28] available in *e.g.* `IMPACT` modeling package.[58] These two approximations are currently also based on the pair-wise sphere-based CFA, Eq. 23. However, unlike the original HCT, the scaling factors that multiply the VDW radii are made explicitly geometry-dependent, rather than set constant. As mentioned above, the scaling of VDW radii is designed to compensate for the over-counting of volume which in the pairwise approximation results from multiple overlaps between atomic spheres. In AGB these overlaps are computed for each pair of atoms; the scaling factors are approximated from two-sphere overlap volumes. For computational efficiency, the atomic volumes are described by Gaussian density functions. Yet another GB flavor based on pair-wise CFA approximation is ACE[25,59] available in *e.g.* TINKER[56] package. The approach uses a set of pre-tabulated atomic volumes—for example Voronoi volumes—to represent the total molecular volume. Each atom's contribution is described by a Gaussian density function which leads to reasonably simple analytical expressions for the integrals in Eq. 23. A completely different approach, not based on the pair-wise approximation and the CFA, is employed by GBMV flavors[43,44] and its variations.[60] Rather than augmenting the VDW representation to approximate the integrals over molecular volume, Lee *et al.* found an analytical approximation of the the appropriate integrals computed over a "smooth boundary" molecular volume that closely mimics the volume used in typical numerical PE calculations. The superior accuracy of these GBMV flavors, relative to the routines based on VDW and pair-wise representations, comes at a price of noticeably higher computational costs.[61]

The above examples represent several important problems and their solutions in the development of the GB field, but by no means give an exhaustive account of all of the variant or "flavors" of the GB model currently available. Among the relatively new developments is "residue pair-wise" GB,[62] the Gaussian GB,[63] and $FACTS$[64] GB flavors. Interestingly, unlike all of the GB flavors discussed above, $FACTS$ approach does not rely on integral representations such as Eqs. 21 to compute the effective radii. Instead, it uses an empirical relationship between the effective radius of an atom and the distribution of other atoms around it. Work to improve the accuracy and efficiency of computational routines for estimation of effective Born radii continues.

2.3 Accounting for salt effects

When salt is present in the solvent, the GB formalism must be amended to include screening effects of the ionic atmosphere. In principle, one could envision repeating the rigorous derivations presented in Section 2.1 starting from the Poisson-Boltzmann equation instead of just the Poisson equation, but to the best of our knowledge the strategy has not yet been carried through. Part of the problem may be that the mathematical structures of the solution of the PB equation inside and outside the dielectric boundary are significantly more complex and substantially different from each other, unlike in the PE case. Instead, the screening effects of monovalent salt are currently introduced into the GB model via an approximate, yet very simple and computationally inexpensive empirical correction[65] to the main formula, Eq. 14:

$$\Delta G_{\mathrm{el}} = -\frac{1}{2}\sum_{i,j}\left(\frac{1}{\epsilon_{\mathrm{in}}} - \frac{exp\left(-0.73\kappa f^{\mathrm{GB}}\right)}{\epsilon_{\mathrm{out}}}\right)\frac{q_i q_j}{f^{\mathrm{GB}}} \tag{24}$$

where $f^{\mathrm{GB}} = \sqrt{r_{ij}^2 + R_i R_j \exp\left(-\gamma \frac{r_{ij}^2}{R_i R_j}\right)}$ as before, and κ is the Debye-Huckel screening parameter $\kappa[\mathring{A}^{-1}] \approx 0.316\sqrt{[\mathrm{salt}][mol/L]}$. The above expression can be rationalized as follows. Notice that the solution of the PB equation for a single point charge has the form $\phi_i \sim \frac{exp(-\kappa r)}{\epsilon_{\mathrm{out}}} \times (\frac{q_i}{r})$, and the role of "$r$" in the GB formula is played by f^{GB}, which suggests the above ansatz $\left(\frac{1}{\epsilon_{\mathrm{in}}} - \frac{1}{\epsilon_{\mathrm{out}}}\right) \rightarrow \left(\frac{1}{\epsilon_{\mathrm{in}}} - \frac{exp\left(-\kappa f^{\mathrm{GB}}\right)}{\epsilon_{\mathrm{out}}}\right)$. The 0.73 prefactor was found empirically to give best agreement with the numerical PB treatment.[65]

2.4 The non-polar contribution

Although the goal of the GB model is to approximate the electrostatic part of solvation only, a comment is due on how the non-polar part is currently handled in practical calculations. A common approximation widely in use today[55] assumes $\Delta G_{\rm nonpolar}$ to be proportional to the total solvent accessible surface area ($\rm SASA$) of the molecule, $\Delta G_{\rm nonpolar} \approx \sigma \times {\rm SASA}$, with the proportionality constant derived from experimental solvation energies of small non-polar molecules. Substantial uncertainty exists in what appropriate value of the surface tension σ should be used in simulations, which perhaps reflects the limitations of this approximation itself. Strong arguments for the use of less drastic approximations for $\Delta G_{\rm nonpolar}$, *e.g.* those that treat solute-solvent van der Waals interactions ("volume term") separately from the surface area term, have also been made.[28,66] Practical models based on these ideas have already emerged. For example, the AGBNP[28] approximation mentioned above combines the basic GB framework with a model for $\Delta G_{\rm nonpolar}$ that goes beyond the surface area approximation.

At the same time, it is clear that, at least in some cases the $\Delta G_{\rm nonpolar} \approx \sigma \times {\rm SASA}$ approximation is not as critical to the over-all accuracy of $\Delta G_{\rm solv}$, compared to the quality of approximating the electrostatic part $\Delta G_{\rm el}$. For example, in a study[25] aimed at assessing the performance of various implementations of the ACE GB flavor in MD simulations of small proteins, it was found that the over-all structural deviations were insensitive to variations of the surface tension σ in a wide range from 0 to $50 cal/mol/\mathring{A}^2$. Some researchers choose to neglect the hydrophobic term altogether in MD simulations, especially if no large conformational changes are expected.

2.5 GB for non-aqueous solvents

To the extent that solvation in non-aqueous media can be attributed to the change in the dielectric properties of the solvent, it is appropriate to seek a modification of the GB formalism to approximate the corresponding $\Delta G_{\rm el}$. In the simplest case of uniform solvent dielectric and arbitrary ratio $\epsilon_{\rm in}/\epsilon_{\rm out}$, one can develop a rigorous formalism similar to the one used to derive the canonical GB model valid in the $\epsilon_{\rm in}/\epsilon_{\rm out} \ll 1$ case, Section 2.1. Namely, the summation of the infinite series that represents the exact Green function for the sphere, Eq. 10, can be performed for any ratio $\epsilon_{\rm in}/\epsilon_{\rm out}$, leading to the following expression:[31]

$$\Delta G_{\rm el} \approx -\frac{1}{2}\left(\frac{1}{\epsilon_{\rm in}}-\frac{1}{\epsilon_{\rm out}}\right)\frac{1}{1+\alpha\beta}\sum_{ij} q_i q_j \left(\frac{1}{f^{\rm GB}}+\frac{\alpha\beta}{A}\right) \quad (25)$$

where $f^{\rm GB}$ is same as above, $\beta=\epsilon_{\rm in}/\epsilon_{\rm out}$, $\alpha=\frac{32(3\ln 2-2)}{3\pi^2-28}-1\approx 0.580127$, and and A is the *electrostatic size* of the molecule. The latter provides a relationship between the molecule's global shape and its electrostatic energy.[31] Roughly speaking, A is the over-all size of the structure; a rigorous definition and a way to compute it analytically is presented in Refs. 31, 35. Whether or not Eq. 25, termed "ALPB" in Ref. 35, can be referred to as a "GB model" may be a matter of debate: unlike the canonical GB formula 14, Eq. 25 contains an extra parameter A and its dependence on the solute and solvent dielectric constants is different. However, the model, currently available in AMBER package, is as efficient computationally as the Still's formula 14 and can also be used in MD simulations[35] to describe solvation effects. Extensive comparisons with the PE reference on realistic biomolecular structures show[31] that the use of Eq. 25 instead of the canonical GB to compute $\Delta G_{\rm el}$ removes a systematic bias present in the canonical GB[35] that becomes especially pronounced outside of the $\epsilon_{\rm in}/\epsilon_{\rm out}\ll 1$ regime.

Despite the simplicity and conceptual appeal of a rigorous physical basis, the ALPB formalism of Eq. 25 has one serious drawback: in its present form it is only applicable to the case of uniform solvent dielectric. To describe the effects of essentially heterogeneous dielectric environment of biological membranes and water/membrane interface, several groups proposed various empirical modifications to the canonical GB. The resulting approximations are currently used in practical simulations of proteins and peptides interacting with biological membranes. The key idea behind these approximations is to keep the main GB formula 25 intact, but to modify the effective Born radii to account for the presence of additional dielectric boundaries. In one such flavor,[67] GBSA/IM (implicit membrane), the membrane is modeled as a homogeneous, low dielectric membrane "slab" that has a finite thickness in one dimension, and extends to infinity in the other two, Fig. 6.

For each atom of the solute, the CFA pair-wise summation in Eq. 23 is then split into two parts: one represents the polarization energy of the atom in the presence of the dielectric slab alone, and the other describes the contribution of the solute atoms outside of the slab. The first contribution is tabulated via a relatively simple

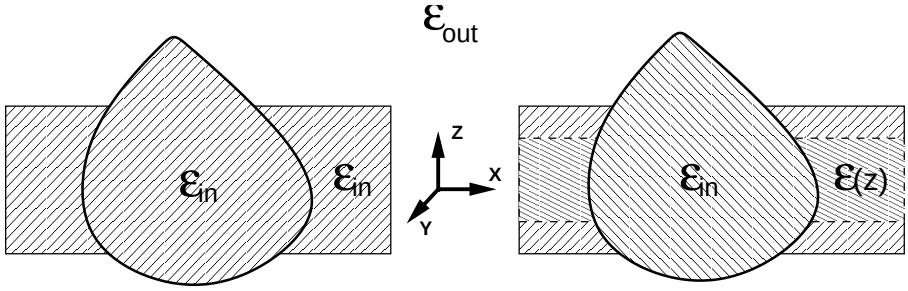

Figure 6: A schematic illustrating two different approaches to approximating the distributions of dielectric in the solute/membrane/solvent system used by some of the available GB flavors to compute the effective Born radii. *Left:* the two-dielectric model used by the GBSA/IM flavor. The low dielectric slab is assumed infinite in the X and Y dimensions. *Right:* the multi-dielectric model of HDGB.

analytical function whose parameters are set by fitting to numerical PE solutions. An obvious limitation of the approach is the assumtion that the membrane environment can be represented by a single dielectric constant which is equal to that of the solute. Recently, the model was modified to account for heterogeneity of the membrane.[68]

A different approach based on the same general idea of incorporating the electrostatic effects of a membrane into appropriately modified effective Born radii was developed in Refs. 60, 69. The resulting heterogeneous dielectric generalized Born (HDGB) flavor is an extension of the GBMV approach discussed above. The first few terms in the infinite series Kirkwood solution 9 were used to suggest a specific form for the self-energy $\Delta G_{ii}^{\rm el}$ as a function of $\epsilon_{\rm in}$ and $\epsilon_{\rm out}$, which in turn is used to modify the original (α_4, α_7)-based GBMV2 expression for the effective Born radii to include an explicit dependence on $\epsilon_{\rm in}$ and $\epsilon_{\rm out}$ in the analytical formula for R_i: $R_i = R_i\epsilon_{\rm in}, \epsilon_{\rm out})$. The theory[69] then proceeds by partitioning the membrane "slab" into several regions of constant dielectric, Fig. 6, approximating a realistic scenario in which the dielectric properties of the membrane vary continuously across the bi-layer. The actual geometry of the slab and the variation of the dielectric constant perpendicular to the membrane plane, $\epsilon(z)$, mimic that predicted for a DPPC bi-layer. This partition is used to define the dielectric environment for each solute atom embedded in the membrane; the corresponding effective radius is computed via the $R_i(\epsilon_{\rm in}, \epsilon_{\rm out})$ prescription. Both GBSA/IM and HDGB flavors are available in CHARMM[70,71] package, along with another membrane-GB flavor based on the same general principle but derived from GBSW mentioned in the previous sections.[72]

3 Applications of the GB model

The algorithmic simplicity and reasonable accuracy of the GB approximation, combined with its availability in popular modeling packages, have made it the method of choice in many practical applications of the implicit solvent methodology. The list is expanding; below are some representative examples.

3.1 Protein Folding and Design

Exploring large conformational transitions is one of several areas where the advantages of implicit solvent framework, and specifically of the GB model, become particularly useful. Recent molecular simulations of the protein folding process, which used all-atom, physics-based potentials to obtain correctly folded structures starting from extended conformations, are arguably one of the most spectacular achievements attributable to the GB model. Examples include small proteins such as 20-residue "trpcage",[73,74] a 23-residue mixed α/β protein,[75] and a 36-residue villin headpiece.[76] Successful folding simulations of even larger proteins are also beginning to appear.[77,78] In these simulations the folded state is typically predicted to within about 2 Å from experiment (C_α rmsd), and in some cases[73,79] within about 1 Å. Energy landscapes computed within the implicit solvent framework were used to gain insights into the folding mechanisms.[76,79] The GB model can also be used to explore the influences of temperature, friction, and random forces on the folding of proteins.[80]

An example of a "protein design" study in which changes of protein stability associated with point mutations were explored with the GB model can be found in Ref. 81. Another relevant example is the use of the model in the prediction of protein loop conformations.[82]

3.2 "Large-scale" motions in macromolecules.

The conformational search speed-up allows one to study large-scale motions in proteins and protein complexes. The use of the methodology to understand large conformational changes in proteins is exemplified by a recent study of the motions of active site flaps in HIV protease:[83] it is unlikely that a comparable explicit solvent study would currently be computationally feasible. Another relevant example is a recent work that explored conformational dynamics of avian flu virus.[84]

Compared to proteins, implicit solvent MD simulations of nucleic acids are relatively new, and not as numerous. A number of methodological issues still need to be resolved. So far, the GB methodology has been employed to model free DNA in solution,[85,86] binding between proteins and nucleic acids,[87–89] as well as for energetic analysis of conformational changes such as the $A \rightarrow B$ transition.[26] A recent all-atom study of the nucleosome and its 147- bp DNA free in solution[90] has demonstrated usefulness of the GB for exploring dynamics of "large" DNA fragments and protein-DNA complexes.

3.3 Peptides and proteins in the membrane environment.

Membranes are large structures, translocation of molecular structures through membranes may involve significant molecular movements and conformational changes, and so these systems are natural candidates for implicit solvent simulations based on the GB model. The GB flavors described in Section 2.5 have been used in modeling of small peptides,[72,91] membrane spanning helices in proteins,[92] and in simulation of whole membrane proteins,[68,69,91] and protein complexes, as large and complex as the bacteriorhodopsin trimer.[93]

3.4 pK prediction and constant pH simulations.

Traditionally, quantitative prediction of pKs and protonation states of ionizable groups in macromolecules has been based on numerical PB solvers, see *e.g.* Refs. 15, 94–97. While development of PB-based approaches for pK prediction continues, GB-based calculations begin to emerge. First applications of the GB model to compute the energetics of proton transfer in proteins were encouraging,[42] although the reference PB calculations were still definitely more accurate. However, a very recent GB-based model for prediction of protein pKs was found competitive with the latest PB-based and empirical approaches.[98]

Up until recently, physics-based pK calculations assumed limited or no coupling between protonation and conformational degrees of freedom. Likewise, charge states of all ionizable groups were considered fixed throughout the course of a typical MD simulation, regardless of the conformational changes that the structure may undergo. In reality, changes in protonation state and conformational changes are strongly coupled. Full and consistent accounting for this coupling may be necessary for further improvement of the accuracy of pK estimates;[99] in dynamics, it may lead to non-trivial effects.[100] The GB model is an ideal candidate to intro-

duce the coupling into dynamical simulations: its instantaneous dielectric response makes possible on-the-fly estimates of relative energies of protonation microstates. Several GB-based approaches have recently been been developed to fully couple protonation and conformational degrees of freedom in molecular dynamics – the so-called *constant pH MD*. One of the methods employs a continuous protonation state model,[101] in which equations of motion are used to time-evolve the protonation coordinate; convergence to physical protonation state of 1 or 0 is enforced by an adjustable potential barrier. An example of recent use of the methodology is a study of pH dependence of folding landscapes of several peptides which provided insights into protein aggregation that occurs in Alzheimer's disease.[102] An alternative approach[103] operates directly in the physical protonation space: protonation states are accepted or rejected on the fly, according to a Metropolis criterion, during the course of the MD simulation. The approach was recently combined with the replica exchange technique to study pH-dependent mechanism of nitric oxide release in nitrophorin proteins.[104] The accuracy of pK predictions based on the constant pH dynamics is becoming competitive[99] with that of the more traditional PB-based models that do not fully account for the structure-protonation coupling.

3.5 Other uses

The use of the GB approximation in molecular modeling is not limited to the general areas outlined above. Applications of the model to the analysis of the energetics of protein-ligand binding have been reported.[45,105–107] Several GB flavors have been implemented in the popular `DOCK` ligand docking program.[108,109] Another emerging area where the GB has been found useful is "hybrid" explicit/implicit approaches to the treatment of the solvent effects. Examples of the latter include a recent model[110] in which the immediate hydration of the solute is modeled explicitly by a layer of water molecules, and the GB model describes the electrostatics of the bulk continuum solvent outside the explicit simulation volume. A similar idea has recently been found very effective in the context of replica-exchange simulations;[111] a detailed account of this methodology can be found in Ref 112. Finally, we will mention recent application of the GB in QM/MM simulations.[113,114]

4 Some practical considerations.

The decision to use the GB approximation instead of the more rigorous PB model or the traditional explicit solvent model may depend on many factors, including the type of molecular structure, specifics of questions one asks of the calculation, and even available computational resources. Which of the numerous GB flavors is an optimal choice for each task also depends on the details. Presented below is a discussion of select aspects of the GB performance in all-atom molecular modeling that is intended to illustrate several general trends backed by specific examples.

4.1 The accuracy/speed trade-offs

One of the main motivations behind developing the GB model has always been its computational efficiency, relative to alternative approximations that describe solvation effects. Since the GB is just an approximation to the more fundamental PB, and both approximations share the same underlying physical framework of the continuum electrostatics, performance comparison between the two models appears natural, though not straightforward in practice. This is because the results may depend on the type of the problem, size and shape of the molecular structure, and also on parameters of the specific algorithms involved, such as grid spacing and specific convergence criteria used in numerical PB solvers. These issues were considered in detail in a recent study[61] which presents a performance comparison between several popular GB models and numerical PB solvers that were commonly available in 2004. The work used the electrostatic solvation energy as the target quantity to assess both accuracy and speed of the models. Not surprisingly, it was found that the most accurate of the GB flavors tested (*e.g.* GBMV and GB^{OBC}) are still less accurate than the most accurate of the PB solvers, but appreciably faster. The difference in speed was up to several orders of magnitude for a small protein (36 residues, 596 atoms), but only about an order of magnitude for a much larger protein (239 residues, 3628 atoms). The trend reflects the difference in scaling behavior between the GB model, which scales with the number of charges as $O(N^2)$ unless further approximations are made, and a more favorable scaling of the PB-based algorithms, *e.g.* $O(N^{3/2})$ for some algorithms that employ successive over-relaxation to solve the finite-difference matrix equations.[115] We stress that the specific trend is only applicable to compact globu-

lar structures such as proteins in their native states; a more detailed discussion of the scaling issues will be presented below in the context of MD simulations. One should also be careful not to over-interpret such comparisons between two different models, and focus on general trends rather than precise numbers. For example, the above mentioned comparison study[61] also found that some of the less accurate numerical PB solvers were quite competitive, speed-wise, with the more accurate GB models. Among the GB flavors, the same general trade-offs were seen: the more accurate approximations were generally slower. For example, the most accurate of the flavors tested in Ref. 61 – GBMV – was found to be several times slower in MD simulations than the next one down the accuracy list, $GB^{OBC}(II)$.

The algorithmic simplicity and computational speed of the GB approximation make it particularly attractive in Molecular Dynamics simulations of biomolecules. Relative to the traditional explicit solvent simulations, the use of the GB model to represent solvation effects can be expected to accelerate the simulation significantly in many cases. The corresponding "speed-up" is the combined effect of two very different contributions: (i) the direct speed-up via reduced computational (clock) time; (ii) the indirect speed-up achieved via enhanced conformational sampling. In what follows we will consider the two contributions separately.

4.2 Computational time relative to explicit solvent

Since MD simulations in explicit solvent require tracking of a large number of water molecules and counterions placed around the solute of interest, one may expect a considerable reduction in CPU (clock) time once this need is eliminated via the use of the GB model. The exact amount of this "direct" relative speed-up is not easy to quantify for the same reasons as in the GB *vs.* numerical PB comparison outlined above: the algorithms to be compared are very different. In explicit solvent simulations, the current practice in the field is to use the so-called Particle Mesh Ewald (PME) approximation[9] to speed up the computation of electrostatic interactions. Within this approach the long-range pair-wise Coulomb interaction energy is represented (via a mathematical trick that relies on imposing artificial periodic boundary conditions on the system) as a sum of rapidly converging series summed in real space, plus a rapidly converging Fourier series. Since both sums converge quickly, an accurate result can be obtained by retaining only a relatively small number of terms in the sums. An additional speed-up comes from the interpolation of the potential over a regular mesh. Several adjustable parameters con-

trol the accuracy and speed of the PME. While any direct comparison of MD simulation timings between the GB and PME is bound to be implementation-dependent, we can still identify several general important trends based on the computational complexity of the two algorithms and types of molecular structures used in the simulations.

The computational complexity of the basic GB equation 14 is obviously $O(N^2_{solute})$, while for the PME it is[9] $O(N_{tot}logN_{tot})$, where N_{solute} is the number of atomic charges in the solute, and N_{tot} is the total number of charges, including those of the solvent, $N_{tot} = N_{solute} + N_{solvent}$. Assuming that one keeps the same thickness of the solvent shell as the size of the solute grows, for *compact globular solutes* and large N_{solute} one has $N_{solvent} \sim N^{2/3}_{solute}, N_{tot} \sim N_{solute}$, and thus the expense of a PME-based computation is effectively $O(N_{solute}logN_{solute})$ for large structures. This means that while a reasonable implementation of the "raw" GB may be expected to be faster than the PME for "small and medium size" structures, the advantage is bound to disappear beyond a certain—implementation dependent—cross-over solute size. We stress that this result assumes no further approximations or algorithmic improvements to the general GB formalism presented in the previous sections.

The above trends for the relative speeds of GB- and PME- computations can be very different for non-compact structures, or simulations where transitions between compact and stretched-out conformations are expected, for example during the process of protein folding. This is because the number of solute molecules required to fill the standard simulation box in these cases will scale differently with the solute size than for the compact globular structures considered above. For example, in the limiting case of a completely stretched-out polymer chain a cubic bounding box, the total volume of the solvent in the box scales as $O(N^3_{solute})$, and hence $N_{total} \sim N^3_{solute}$, which leads to $O(N^3_{solute}logN_{solute})$ for the PME computational complexity, compared to just $O\left(N^2_{solute}\right)$ of the "raw" GB. Thus, in contrast to the case of compact globular structures, GB-based simulations of extended conformations are always expected to be considerably less expensive than the corresponding explicit solvent computations that employ the PME.

We now illustrate the above general trends on concrete examples. We will compare single CPU timings between the GB^{OBC} flavor and the PME, in MD simulations of a set of proteins in their compact, native states. For this illustration we will be using the models implemented in a popular MD package AMBER (8).[55]

Unless otherwise specified, we choose the default values for the input parameters such as non-bonded cut-off (9 Å) in PME. The solvent buffer size is 10 Å . No long-range cut-offs or other approximations will be applied in the GB-based simulations. The results of the comparison are as follows. For a small protein villin headpiece (36 residues, 596 atoms), a GB-based simulation proceeds roughly ten times faster than the corresponding explicit solvent one based on the PME. The timings become about equal for a medium-size protein ubiquitin (76 residues, 1231 atoms). For a much larger nucleosome structure (8 protein subunits + 146 base-pairs of DNA, about 25,000 atoms in total) it was found earlier[90] that the ratio of computational times is about $10 : 1$ in favor of the PME, although parameters of that specific simulation were somewhat different from those used in the single protein examples. Thus, for these specific GB and PME implementations used to compute electrostatic interactions in all-atom MD simulations of compact globular structures, the cross-over size beyond which the PME-based simulation becomes faster than those based on the GB is somewhere between 1000 and 2000 atoms. Note that this result applies to simulations that use a single CPU. The cross-over point may be effectively pushed towards larger structures if one has access to a multi-CPU cluster: the GB-based simulations generally tend to scale better with the number of utilized processors than the PME-based ones. Recent AMBER (version 9) benchmarks provide some concrete examples: for structures of about 25,000 atoms, the maximum speed-up – that is the speed-up beyond which doubling the number of CPUs does not lead to any significant increase in compute speed – is at least 7 times higher for the GB-based simulations than for the PME-based runs. Thus, relative computational speed of the GB model can be substantially increased, albeit extensively, if one has an access to a large parallel machine. The use of graphics processing units (GPU) to speed-up GB-based molecular dynamics calculations may also holds considerable promise. For example, a recent study demonstrated that a two orders of magnitude acceleration vs. a single CPU can be achieved for a $\sim 5,000$ atom protein in an all-atom molecular dynamics running entirely on a GPU.[116]

Additional approximations can also be used to reduce the associated direct simulation costs in GB-based simulations.* For example, the latest versions of AMBER offer at least three different strategies to speed up such simulations: some of these strategies are specific to the GB methodology and some are generic and have been used in the explicit solvent simulations as well. Among the latter is the *multiple step* approach in which

*Note that the now standard PME approach is not applicable to GB, at least in its current form.

slow-varying long range forces are not calculated at every step of MD, but only every `nrespa` > 1 steps. In addition, the standard long range cut-off schemes may be very useful in GB-based simulations. The cut-off schemes have become almost obsolete in explicit solvent MD in part due to success of the Ewald method and in part since it became evident that spherical cut-offs introduce artifacts into explicit solvent simulations,[117] affecting particularly strongly the structure and dynamics of water. However, the very absence of explicit water in the GB-based simulations may make them more amenable to long-range cut-offs— successful long MD runs have been reported using cut-off values of 24,[45] 18,[85] or even 12[88] Å . While for small systems the benefits of using realistic cut-offs are not very high, the speed-ups may become significant for larger molecules where a reasonable cut-off may be chosen to be considerably smaller than the system size. The specific numbers will necessarily be implementation-dependent. Also, one should always be aware that spherical cut-offs may not be appropriate for highly charged systems or other situations where long-range electrostatic interactions play a key role, such as in nucleic acids or the nucleosome. Fortunately, yet another way to cut GB computational expense is now available which is based on reducing the cost of computing the effective Born radii. This is achieved by setting a finite upper limit, `rgbmax` , in the integral Eq. 20, so that only the part of the solvent within the `rgbmax` around the given atom is taken into account in computing its effective radius. Atoms whose associated spheres are farther away than `rgbmax` from the given atom will not contribute to that atom's effective Born radius. This is implemented in a "smooth" fashion[118] so that when part of an atom's sphere lies inside the `rgbmax` sphere, that part still contributes to the low-dielectric region that determines the effective Born radius. As a result, the derivatives of the total energy with respect to atomic coordinates are continuous, leading to energy conservation, and there is no large spurious force acting on the atoms coming in and out of this "reaction field cut-off". Importantly, unlike in the case of the standard cut-off, even if two charges are separated by a distance larger than `rgbmax` they still interact, albeit with a somewhat altered strength.

The implicit solvent methodology is relatively new, and so studies on speeding up MD simulations based on it are not nearly as many or extensive as is the case with the explicit solvent MD. However, the limited available evidence is encouraging. For example,[118] MD simulations of several small and medium size proteins, 10 bp duplexes of B-DNA and RNA have shown that, at least on the time-scales of up to 10 ns, the use of `rgbmax` preserves the native structure to the same extent as do simulations in which this approximation was

Table 1: The effect of several additional approximations on the speed and accuracy of GB-based MD simulations. Shown are the deviations from the native structure (backbone rmsd, Å) and relative computational speed-up for a set of 8 ns. long MD simulations of a 76-residue protein ubiquitin (PDB 1UBQ), all done with $GB^{\rm OBC}$ model (`igb` = 5) of `AMBER` . Further details of the MD protocol can be found in Ref. 45. In simulations that employed the multiple time-step algorithm, that is recomputed the long-range forces only at every `nrespa` > 1 step, Langevin dynamics was used. The collision frequency was set to a low value of `gamma_ln` = 0.05 ps^{-1}. The average and max. values of the rmsd were computed over the entire trajectory in each case. The value of long-range cut-off is specified by `cut`.

`rgbmax`	`cut`	`nrespa`	$\langle$rmsd$\rangle$	max rmsd	relative direct speed-up
40	40	1	1.05	1.6	1
40	18	1	1.3	2.0	1.1
9	40	1	1.1	1.8	1.6
9	18	1	1.28	2.11	1.9
40	40	4	1.6	2.5	2.4
9	40	4	1.23	2.1	4.0
9	18	4	1.08	2.08	4.4

not used, as in Ref. 45. Even fewer tests have been performed that examine the effects of multiple time step approximation in implicit solvent MD, or a combination of it with the traditional spherical cut-off and/or the use of `rgbmax` . Still, the limited experience we have is encouraging, see Table 1, where we have summarized the results of applying such approximations in MD simulations of a 76-residue protein.

A conclusion can be drawn that at least for this particular protein the use of any of the algorithmic improvements described above brings about a speed-up, with only modest disruption of the native structure of the protein. When two or more of the methods are combined, their speed-ups combine too, though not necessarily in a linear fashion: the use of reasonable values of `rgbmax` , the long-range cut-off `cut` , and multiple time-steps `nrespa` together (last row in Table 1) results in a 4-fold increase in computational speed compared to the simulation in which none of the methods have been used (first row). The algorithmic improvements discussed above are expected to be even more efficient for larger systems. For example, our recent experience[90] with the GB-based MD simulations of the nucleosome core particle ($\sim$ 25,000 atoms, system size $\sim$ 120 Å) shows that the use of `rgbmax` = 15 Å results in about three-fold increase in speed for the system, while yielding stable trajectories. Even with `rgbmax` = 40 Å , the speed up was still more than two-fold. Note that the use of the standard long-range cut-off would be problematic for this highly charged compound. At the same

time, it is clear that the more of the additional approximations are made, the larger are the deviations from the native structure, and so one has to be very cautious, especially in the yet unexplored regimes. It is also worth mentioning that, compared to the standard explicit solvent simulations, more careful multi-step equilibration protocols may be necessary in the regime where solvent viscosity is considerably reduced or even set to zero.[45] Over-all, based on admittedly very limited evidence, we conclude that the three approximations to speed-up the GB-based simulations yield encouraging results, suggesting that these are worth exploring further. Development of novel approximations that promise to bring computational complexity of the GB model to $O(NlogN)$ is underway.[119]

4.3 Enhancement of conformational sampling

This is one of the most significant advantage that the GB model has to offer, although a quantitative analysis of the effect and its relative contribution to the corresponding "indirect" speed-up of the GB-based MD simulations is even less straightforward than for the "direct" speed-up considered above. Part of the difficulty is that the sampling enhancement depends on many details of the molecular system and the process studied, and may also depend on the specifics of the GB model and MD algorithms used. Below we will present a few semi-quantitative and qualitative observations based on the limited data available in literature.

One can make estimates of the degree of conformational sampling enhancement by comparing kinetics of specific conformational transitions in the implicit and the corresponding explicit solvent simulations. Generally, the enhancement of conformational sampling can be thought of as a combination of at least two effects: increased sampling due to significant reduction or complete elimination of solvent viscous forces that slow down the motion of the solute parts, and faster conformational search due to the effective smoothing of energy landscapes. The interplay of these effects in GB-based MD simulations of small model systems have recently been considered in detail by Hamelberg *et al.*[120] and Feig,[121] for specific GB models in AMBER (GB^{OBC}) and CHARMM (GBMV) respectively. Relevant discussions more focused on the GB-based protein folding simulations can also be found in Refs. 76, 80.

Hamelberg *et al.* reported a 10^4 increase in the rate of conformational sampling due to the combined effect of both the landscape smoothing and reduced solvent viscosity, as assessed by comparing the $cis \leftrightarrow$

$trans$ isomerization rate in a di-peptide relative to the corresponding rate in explicit water simulations. When the solvent viscosity was increased to the levels corresponding to that of water, by appropriately increasing the collision frequency in Langevin dynamics, the isomerization rate was still found to be about one to two orders of magnitude higher than that in explicit water. Thus, in this specific model and molecular system, 2 to 3 orders of magnitude enhancement of sampling relative to explicit solvent comes from the elimination of solvent viscous forces and the remaining 2 to 1 orders of magnitude are due to the smoothing of the energy landscape. Thus, it is reasonable to assume that the elimination/reduction of solvent viscosity alone should result in significant effective speed-up of viscosity-controlled conformational transitions. We hypothesize that this type of transitions is likely to involve large-scale relative motions of parts of the structure along a relatively smooth energy landscape. This hypothesis may explain the significant folding rate enhancement observed in the GB-based MD simulations of folding of some small proteins. For example, note that experimental folding times for even the fastest folding proteins is of the order of microseconds, whereas in some of the GB-based protein folding simulations[73] described in the previous sections the native state was reached on 10 ns time-scale. Assuming that the folding rates in explicit solvent are the same order of magnitude as the experimental ones, the comparison gives a very rough idea of the magnitude of conformational search speed-ups—at least two orders of magnitude—that one can expect in these types of simulations through the use of the GB model. We emphasize that the specific numbers may only be applicable to the GB flavors (`AMBER`) used in these simulations, see below. For a relevant general discussion of the interplay of time-scales and friction forces in protein folding, see *e.g.* Ref. 122; a detailed analysis of the folding rate dependence on viscous effects for 20-residue protein is available Ref. 76.

The magnitude of the conformational search speed-up relative to the explicit solvent also depends on the type conformational rearrangements. In a GB-based simulation of $A \leftrightarrow B$ transition in DNA, Tsui *et al.*[26] reported only a ~ 20 fold increase in the transition speed. We do not know whether the more modest transition rate enhancement observed in this system is indeed due to the fact that the transition involves relatively smaller structural rearrangements and higher barriers, but it is a plausible hypothesis. A similar amount of a conformational sampling speed-up was estimated from an analysis of open/close loop transition events in the avian flu virus protein.[84] On the other hand, global bending of the DNA on length-scales comparable to its persistence

length appears to occur about a 100 times faster in GB-based simulations[90] relative to explicit solvent.[123] This amount of conformational sampling enhancement is more consistent with viscosity-controlled dynamics.

Over-all, while there is no doubt that the use of the GB-model to represent solvation effects in simulations does bring about appreciable increase in the rate of conformational sampling in many cases, the precise magnitude of this increase depends strongly on the specifics of the system and processes under study. The rate increase also appears to depend of the particular implicit solvent model. For example, in contrast to the numbers discussed above appropriate for the GB flavors in `AMBER`, considerably smaller acceleration of conformational sampling— only about a factor of 4 to 5— was observed[121] with a GBMV flavor available in `CHARMM`. Moreover, the zero solvent viscosity limit achieved in the absence of stochastic collisions with the solute (via the use of Nosé-Hoover thermostat) actually *slowed down* conformational transitions in alanine di-peptide in that study, relative to the explicit solvent. At least some of the slow-down in this case was attributed to the lack of thermal "jolts" from stochastic collisions that help cross potential barriers.

5 Limitations of the GB model.

The generalized Born model is separated from reality by several layers of approximations, Fig. 7, each of them adding its own limitations to the method. Some of these limitations directly affect the accuracy of the GB approximation, while others may simply restrict its areas of application. For example, no matter how accurate a specific flavor of the GB model may be, continuous electrostatic potential can not be defined within its context: at best one can talk about potential at atomic centers only.[42] Thus, unlike the PB model, the GB approximation proper can not be used to produce the colorful distributions of electrostatic potential that are now widely used in structural biology. To have this specific capability within an analytical model one has to go beyond the GB.[32,124]

More important, however, are limitations that directly affect the accuracy of the GB relative to the more fundamental descriptions of solvation, such as the explicit solvent framework or the PB model.

The most fundamental approximation step, the "discrete → continuum" approximation obviously eliminates a number of real solvent effects that depend on the finite size of the water molecule, such as de-wetting.

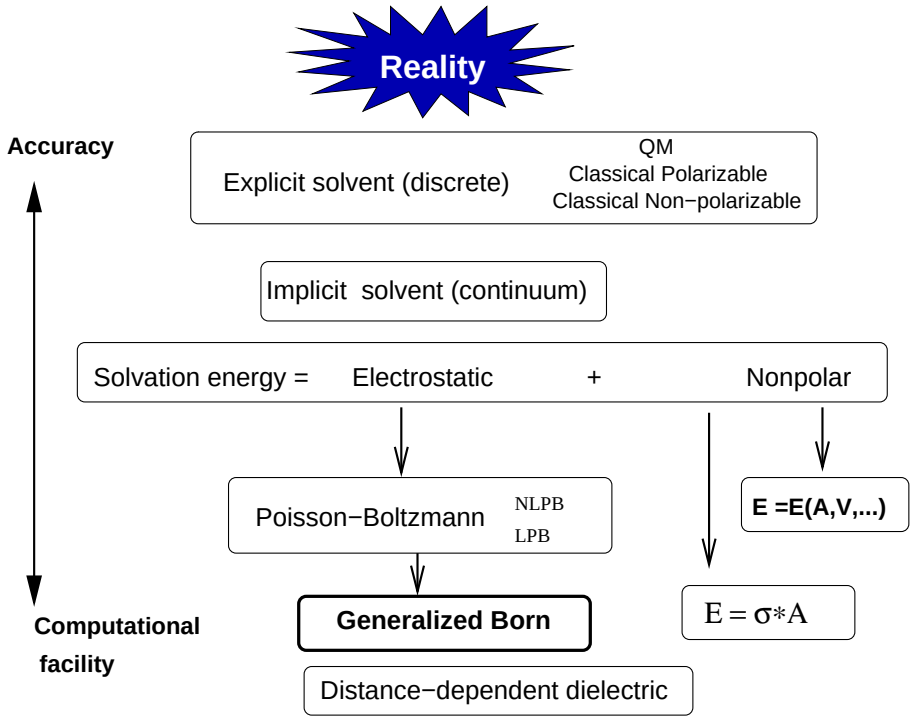

Figure 7: The hierarchy of representations of solvent effects in molecular modeling. The GB model is separated from reality by several layers of approximation.

Likewise, the implicit solvent model cannot describe effects of tightly bound water molecules, which may be a serious limitation when those are important for function or stability of the structure of interest. For example, in protein-ligand complexes structured water is sometimes found right at the binding interface. Also, it is not clear how well the continuum approximation works inside deep binding pockets, where solvent can hardly be considered as having properties of the bulk. Water–solvent hydrogen bonds are present in the implicit solvent model only approximately, at a mean-field level, which may under- or over- estimate their strengths in specific cases.

The Poisson-Boltzmann approximation inherits the above generic limitations of mean-field theories and linear response approximations, and adds its own. In particular, the neglect of correlation between counterions, especially multi-valent ones such as Mg^{2+}, may be a serious problem in the modeling of highly charged structures such as nucleic acids. The $PB \rightarrow GB$ step introduces several additional approximations. Earlier GB models, as well as models that used uncorrected pairwise schemes based on VDW atom spheres to compute the effective radii, could be expected to perform worse on larger structures relative to small molecules, see the

discussion in Section 2.2.2. Fortuitous cancellation of errors often masked this problem in calculations of the total electrostatic solvation energy.[38] The latest generations of the GB models have overcome some of these problems. Still, from the derivation of the GB model presented in Section 2.1, it can be expected that for a given structure the largest errors relative to the PB treatment will occur in regions whose local shapes deviate most from spherical. The heuristic correction in the Still's formula that partially accounts for deviations of molecular shape from a perfect sphere is uncontrollable. It is unrealistic to expect that its effect on the over-all accuracy, even relative to the PB, would be exactly quantifiable *a-priori* for any biomolecular simulation.

An additional complication is that while there is really only one GB model, any of its practical applications relies on a specific flavor of the model. There is now well over ten such flavors, and the number is alarmingly on the rise, especially if one counts in the numerous parametrizations of the same basic "flavor". There is enough difference between most of these flavors and their detailed parametrizations[74] that specific results obtained with one flavor/parametrization can not necessarily be expected to be reproducible with another. This is particularly true in dynamical applications. Note that in this case it is not only the specifics of the GB flavor that affect the outcome, but also the way the non-polar contribution is computed. The choice of underlying gas-phase force-field is also important: one can not automatically assume that a force-field known to outperform its predecessor within the explicit solvent framework will also show better performance when used with a given GB model.[125] Here, by "performance" we mean agreement with the explicit solvent and/or experiment.

Even though it may not be possible to make an unambiguous choice of the best performing combination of GB flavor and gas-phase force-field, one general trend appears to emerge. The latest GB flavors that show better agreement with the underlying PB model are likely to perform better than older flavors that did not agree with the PB all that well. Since the PB is also an approximation, a natural question is then how much of the error seen in GB-based MD simulations is already present at the PB level? For example, it appears that at least some of the GB flavors do not have the right balance between intra-solute and solvent-solute charge-charge interactions, resulting in over-stabilization of solvent exposed salt bridges.[126] However, a careful follow-up study revealed that not all of the discrepancy (with the reference explicit solvent results) came from the GB model, with some of it being inherent to the PB. Importantly, even the use of "perfect"[38] effective radii in the GB Eq. 14 does not match the accuracy of the PB in predicting relative energies of conformational states of

small peptide, see Ref. 127 for important details. In this particular study, the error of the PB itself, relative to explicit solvent treatment, was found to be smaller, but not negligible compared to the GB error. Thus, there still appears to be room for improvement within the $PB \rightarrow GB$ approximation.

6 Conclusions and outlook

Within the implicit solvent framework, solvation effects are modeled by replacing individual solvent molecules with a continuous medium that mimics bulk properties of the solvent. Even though the framework makes several fundamental approximations to reality, it is an attractive alternative to the more conventional explicit representation which track movements of discrete solvent molecules. Practical models based on the implicit solvent framework, such as the GB model considered here, offer several significant advantages over the explicit water representation, including lower computational costs, faster conformational search, and very effective ways to estimate relative free energies of conformational ensembles.

The generalized Born (GB) model provides a simple analytical formula for molecular electrostatic energy in the presence of implicit solvent. In the hierarchy of approximations that lead to model, the GB lies below the more fundamental model based on the Poisson equation (PE) of continuum electrostatics. In fact, apart from a heuristic correction term, the general mathematical form of the GB corresponds to the exact PE result for the electrostatic part of solvation free energy for a hypothetical perfectly spherical molecule surrounded by uniform dielectric medium in the conductor limit (infinitely high dielectric). Heuristic corrections partially account for realistic biomolecular shapes, screening effects of monovalent salt, and high, but finite dielectric of water. Non-homogeneous dielectric environments such as biological membranes require additional corrections. The accuracy of the GB model depends critically on the accuracy of the so-called effective Born radii that characterize positions of each partial atomic charge relative to molecular surface of the structure. Many practical algorithms for computing the effective radii have been developed, leading to the many different "flavors" of the basic GB model available today. Expected trade-offs between accuracy and speed apply. The accuracy of the effective radii depend largely on how realistic is the representation for the solvent/solute dielectric boundary used by the specific algorithm: simplified representations are typically more facile computationally, but lead to

less accurate radii.

In several applications such as molecular dynamics simulations where robustness of the algorithms and computational efficiency are of paramount concerns, the generalized Born (GB) model has arguably become the most widely used approximation for molecular electrostatic energy in the presence of implicit solvent. Perhaps one of the most spectacular achievements of the model is the successful first-principles (physics-based) simulations of the complete folding process of several small proteins at full atomic level – a fit that is probably not yet within reach for the corresponding all-atom explicit solvent simulations. Other areas where the model's effectiveness is found particularly useful include exploration of large-scale motions in proteins or DNA, protein design, modeling of the membrane environment, and replica-exchange simulations based on novel "hybrid" explicit/implicit approaches. For some types of calculations, *e.g.* constant pH molecular dynamics, models based on implicit solvation such as the GB appear to be the only ones currently available in practice. Recently, encouraging results have also been obtained in applying the GB model for prediction of pK shifts in proteins, QM/MM simulations, and in the field of protein-ligand docking. While there is no doubt at the moment that use of the implicit solvent in molecular simulations may bring considerable rewards, it is also associated with additional uncertainty compared to the more traditional calculations based on the explicit solvent. Less is known about the domain of applicability of the implicit solvent framework, and so extra care must be taken when using practical models based on it, including the GB. The decision of whether or not the potential rewards of using the GB model are likely to outweigh the risks depend on many factors. These may include type of molecular structure, specifics of the questions one asks of the calculation, and even available computational resources. For example, the task of exploring large conformational changes in a protein is a good candidate for GB-based simulations, especially on a parallel machine. At the same time, if one simply needs to generate an ensemble of near native conformations of the same protein on a PC, then the tried-and-true explicit solvent approach (with the electrostatics treated by PME) is probably a better choice. Once the decision of using the GB model is made, the researcher is typically faced with many additional practical issues, including choice of optimal GB flavor for the specific task at hand. As we have seen above, the flavors may differ substantially in their accuracy and speed, including the speed of conformational sampling which may be a critical factor in making the choice. An additional complication is that many of the GB flavors available in popular modeling

packages deliver optimal performance only in conjunction with a specific gas-phase force-field, including the associated atomic radii sets used in the calculation of the effective Born radii.

Despite many documented successes of the GB model, situations where it clearly needs improvement are abundant. These help establish boundaries of applicability of the currently available GB flavors; they also suggest directions for future improvements of the model. These improvements will likely include progress in the following areas:

(i) Systematic quantitative exploration of performance of the available GB flavors. Development of comprehensive consensus test sets and practices.

(ii) Further parameter optimization of the most promising of the existing GB flavors against the PB and explicit solvent. The challenge here is not to over-parametrize the GB model beyond its natural accuracy limits. Transferability of the highly parametrized solutions will probably remain problematic.

(iii) Development and testing of novel ways to compute the effective Born radii such as the "R6" prescription that yields exact effective radii in the perfect spherical case. The method is appealing from both the accuracy and computational facility standpoints, but it remains to be seen how its practical implementations will perform.

(iv) Development of novel approaches designed specifically to reduce computational complexity of GB-based molecular simulations, ideally to $O(NlogN)$, without the loss of accuracy associated with the traditional spherical cut-off schemes.

(v) Revision of the theoretical foundation of the GB model aimed at bringing its accuracy closer to the more fundamental PB model, while preserving the appealing simplicity of the canonical GB. It is apparent now that the Still's formula has reached its accuracy limits, but developing a superior approximation that is equally simple and robust is probably the most challenging task on the list above.

7 Acknowledgments

The author thanks Andrew Fenley and Ramu Anandakrishnan for reading the manuscript and making helpful suggestions. Financial support from the NIH (R01 GM076121) is acknowledged.

8 Bibliography

1. Cramer, C. J. and Truhlar, D. G. Implicit Solvation Models: Equilibria, Structure, Spectra, and Dynamics. Chem. Rev. 99:2161–2200, 1999.

2. Honig, B. and Nicholls, A. Classical Electrostatics in Biology and Chemistry. Science 268:1144–1149, 1995.

3. Beroza, P. and Case, D. A. Calculation of Proton Binding Thermodynamics in Proteins. Methods Enzymol. 295:170–189, 1998.

4. Madura, J. D., Davis, M. E., Gilson, M. K., Wade, R. C., Luty, B. A., and McCammon, J. A. Biological Applications of Electrostatic Calculations and Brownian Dynamics. Rev. Comp. Chem. 5:229–267, 1994.

5. Gilson, M. K. Theory of Electrostatic Interactions in Macromolecules. Curr. Opin. Struct. Biol. 5:216–223, 1995.

6. Scarsi, M., Apostolakis, J., and Caflisch, A. Continuum Electrostatic Energies of Macromolecules in Aqueous Solutions. J. Phys. Chem. A 101:8098–8106, 1997.

7. Luo, R., David, L., and Gilson, M. K. Accelerated Poisson-Boltzmann calculations for static and dynamic systems. J. Comp. Chem. 23:1244–1253, 2002.

8. Sagui, C. and Darden, T. A. Molecular dynamics simulations of biomolecules: long-range electrostatic effects. Annu Rev Biophys Biomol Struct 28:155–179, 1999.

9. Schlick, T. Molecular Modeling and Simulation. Springer, , 2002.

10. Mobley, D. L., Ii, A. E., Fennell, C. J., and Dill, K. A. Charge asymmetries in hydration of polar solutes. J Phys Chem B 112(8):2405–2414, Feb, 2008.

11. Lazaridis, T. and Karplus, M. Effective energy function for proteins in solution. Proteins 35(2):133–152, May, 1999.

12. Dzubiella, J., Swanson, J. M., and McCammon, J. A. Coupling nonpolar and polar solvation free energies in implicit solvent models. J Chem Phys 124(8), February, 2006.

13. Kirkwood, J. G. Theory of Solution of Molecules Containing Widely Separated Charges with Special Application to Zwitterions. J. Chem. Phys. 2:351–361, 1934.

14. Frank-Kamenetskiĭ, M. D., Anshelevich, V. V., and Lukashin, A. V. Polyelectrolyte model of DNA. Sov. Phys. Usp. 30(4):317, Apr, 1987.

15. Bashford, D. and Karplus, M. pK_{a}s of Ionizable Groups in Proteins: Atomic Detail from a Continuum Electrostatic Model. Biochemistry 29:10219–10225, 1990.

16. Sharp, K. A. and Honig, B. Electrostatic Interactions in Macromolecules. Ann. Rev. Biophys. Biophys. Chem. 19:301–332, 1990.

17. Baker, N. A., Sept, D., Joseph, S., Holst, M. J., and McCammon, J. A. Electrostatics of nanosystems: application to microtubules and the ribosome. Proc Natl Acad Sci U S A 98(18):10037–10041, Aug, 2001.

18. Rocchia, W., Alexov, E., and Honig, B. Extending the applicability of the nonlinear poisson-boltzmann equation: Multiple dielectric constants and multivalent ions. J. Phys. Chem. B 105(28):6507–6514, July, 2001.

19. Nicholls, A. and Honig, B. A Rapid Finite Difference Algorithm, Utilizing Successive Over Relaxation to solve the Poisson-Botzmann Equation. J. Comp. Chem. 12:435–445, 1991.

20. Simonson, T. Electrostatics and Dynamics of Proteins. Rep. Prog. Phys. 66:737–787, 2003.

21. Baker, N., Bashford, D., and Case, D. Implicit solvent electrostatics in biomolecular simulation. In *New Algorithms for Macromolecular Simulation*, volume 49 of *Lecture Notes in Computational Science and Engineering*, 263–295. Springer, , 2006.

22. Baker, N. A. Improving implicit solvent simulations: a poisson-centric view. Curr Opin Struct Biol 15(2):137–143, Apr, 2005.

23. Dominy, B. N. and Brooks, C. L. Development of a Generalized Born Model Parametrization for Proteins and Nucleic Acids. J. Phys. Chem. B 103:3765–3773, 1999.

24. Bashford, D. and Case, D. Generalized Born models of macromolecular solvation effects. Annu. Rev. Phys. Chem. 51:129–152, 2000.

25. Calimet, N., Schaefer, M., and Simonson, T. Protein molecular dynamics with the generalized born/ace solvent model. Proteins: Structure, Function, and Genetics 45(2):144–158, 2001.

26. Tsui, V. and Case, D. Molecular dynamics simulations of nucleic acids using a generalized Born solvation model. J. Am. Chem. Soc. 122:2489–2498, 2000.

27. Wang, T. and Wade, R. Implicit solvent models for flexible protein-protein docking by molecular dynamics simulation. Proteins 50:158–169, 2003.

28. Gallicchio, E. and Levy, R. M. AGBNP: an analytic implicit solvent model suitable for molecular dynamics simulations and high-resolution modeling. J. Comp. Chem. 25:479–499, 2004.

29. Nymeyer, H. and Garcia, A. E. Free in PMC simulation of the folding equilibrium of alpha-helical peptides: a comparison of the generalized Born approximation with explicit solvent. Proc. Natl. Acad. Sci. U. S.Ȧ. 100:13934–13949, 2003.

30. Jackson, J. D. Classical Electrodynamics. J. Wiley & Sons, New York, , 1975.

31. Sigalov, G., Scheffel, P., and Onufriev, A. Incorporating variable dielectric environments into the generalized Born model. J Chem Phys 122(9):094511–094511, Mar, 2005.

32. Fenley, A. T., Gordon, J. C., and Onufriev, A. An analytical approach to computing biomolecular electrostatic potential. i. derivation and analysis. The Journal of Chemical Physics 129(7):075101, 2008.

33. Grycuk, T. Deficiency of the Coulomb-field approximation in the generalized Born model: An improved formula for Born radii evaluation. The Journal of Chemical Physics 119(9):4817–4826, Sep, 2003.

34. Still, W. C., Tempczyk, A., Hawley, R. C., and Hendrickson, T. Semianalytical Treatment of Solvation for Molecular Mechnics and Dynamics. J. Am. Chem. Soc. 112:6127–6129, 1990.

35. Sigalov, G., Fenley, A., and Onufriev, A. Analytical electrostatics for biomolecules: beyond the generalized Born approximation. J Chem Phys 124(12):124902–124902, Mar, 2006.

36. Hoijtink, G. J., E, B. D., Van Der Meij, P. H., and Weijland, W. Reduction potentials of various aromatic hydrocarbons and their univalent anions. Recueil des Travaux Chimiques des Pays-Bas 75:487–503, 1956.

37. Constanciel, R. and Contreras, R. Self consistent field theory of solvent effects representation by continuum models: Introduction of desolvation contribution. Theoretica Chimica Acta 65(1):1–11, 1984.

38. Onufriev, A., Case, D. A., and Bashford, D. Effective Born radii in the generalized Born approximation: the importance of being perfect. Journal of Computational Chemistry 23(14):1297–304, Nov, 2002.

39. Hawkins, G. D., Cramer, C. J., and Truhlar, D. G. Pairwise solute descreening of solute charges from a dielectric medium. Chem. Phys. Lett 246:122–129, 1995.

40. Hawkins, G. D., Cramer, C. J., and Truhlar, D. G. Parametrized models of aqueous free energies of solvation based on pairwise descreening of solute atomic charges from a dielectric medium. J. Phys. Chem. 100:19824–19836, 1996.

41. Scarsi, M., Apostolakis, J., and Caflisch, A. Continuum electrostatic energies of macromolecules in aqueous solutions. Journal of Physical Chemistry A 101(43):8098–8106, Oct, 1997.

42. Onufriev, A., Bashford, D., and Case, D. A. Modification of the generalized Born model suitable for macromolecules. The Journal of Physical Chemistry B: Condensed matter, materials, surfaces, interfaces and biophysical chemistry 104(15):3712–3720, Apr, 2000.

43. Lee, M. S., F. R. Salsbury, J., and Brooks, III, C. L. Novel generalized Born methods. J. Chem. Phys. 116:10606–10614, 2002.

44. Lee, M. S., Feig, M., Salsbury, F. R., and Brooks, C. L. New analytic approximation to the standard molecular volume definition and its application to generalized Born calculations. Journal of Computational Chemistry 24(11):1348–56, Aug, 2003.

45. Onufriev, A., Bashford, D., and Case, D. A. Exploring protein native states and large-scale conformational changes with a modified generalized Born model. Proteins 55(2):383–94, May, 2004.

46. Ghosh, A., Rapp, C. S., and Friesner, R. A. Generalized born model based on a surface integral formulation. J. Phys. Chem. B 102:10983–10990, 1998.

47. Romanov, A. N., Jabin, S. N., Martynov, Y. B., Sulimov, A. V., Grigoriev, F. V., and Sulimov, V. B. Surface Generalized Born Method: A Simple, Fast, and Precise Implicit Solvent Model beyond the Coulomb Approximation. Journal of Physical Chemistry A 108(43):9323–9327, Oct, 2004.

48. Lee, M. S., Salsbury, F. R., and Brooks, C. L. Novel generalized Born methods. The Journal of Chemical Physics 116(24):10606–10614, Jun, 2002.

49. Mongan, J., Svrcek-Seiler, W. A., and Onufriev, A. Analysis of integral expressions for effective born radii. J Chem Phys 127(18):185101–185101, Nov, 2007.

50. Im, W., Beglov, D., and Roux, B. Continuum solvation model: Computation of electrostatic forces from numerical solutions to the poisson-boltzmann equation. Computer Physics Communications 111(1-3):59–75, June, 1998.

51. Swanson, J. M. J., Mongan, J., and McCammon, J. A. Limitations of Atom-Centered Dielectric Functions in Implicit Solvent Models. The Journal of Physical Chemistry B: Condensed matter, materials, surfaces, interfaces and biophysical chemistry 109(31):14769 –14772, Aug, 2005.

52. Im, W., Lee, M. S., and Brooks, C. L. Generalized born model with a simple smoothing function. Journal of computational chemistry 24(14):1691–1702, November, 2003.

53. Tjong, H. and Zhou, H. X. GBr6: A parameterization-free, accurate, analytical generalized born method. J. Phys. Chem. B 111(11):3055–3061, March, 2007.

54. Labute, P. The generalized born/volume integral implicit solvent model: Estimation of the free energy of hydration using london dispersion instead of atomic surface area. Journal of Computational Chemistry 29:1693–1698, 2008.

55. Case, D. A., Cheatham, T. E., Darden, T., Gohlke, H., Luo, R., Merz, K. M., Onufriev, A., Simmerling, C., Wang, B., and Woods, R. J. The Amber biomolecular simulation programs. J Comput Chem 26(16):1668–1688, Dec, 2005.

56. Ponder, J. In *TINKER: Software Tools for Molecular Design, 3.9.* Washington University School of Medicine, Saint Louis, MO, , 2001.

57. Mongan, J., Simmerling, C., McCammon, J., Case, D., and Onufriev, A. Generalized born model with a simple, robust molecular volume correction. J. Chem. Theory and Comput. 3:156–169, 2007.

58. Banks, J. L., Beard, H. S., Cao, Y., Cho, A. E., Damm, W., Farid, R., Felts, A. K., Halgren, T. A., Mainz, D. T., Maple, J. R., Murphy, R., Philipp, D. M., Repasky, M. P., Zhang, L. Y., Berne, B. J., Friesner, R. A., Gallicchio, E., and Levy, R. M. Integrated modeling program, applied chemical theory (impact). Journal of Computational Chemistry 26(16):1752–1780, 2005.

59. Schaefer, M. and Karplus, M. A Comprehensive Analytical Treatment of Continuum Electrostatics. J. Phys. Chem. 100:1578–1599, 1996.

60. Feig, M., Im, W., and Brooks, C. L. Implicit solvation based on generalized Born theory in different dielectric environments. J. Chem. Phys. 120(2):903–911, January, 2004.

61. Feig, M., Onufriev, A., Lee, M. S., Im, W., Case, D. A., and Brooks, C. L. Performance Comparison of Generalized Born and Poisson Methods in the Calculation of Electrostatic Solvation Energies for Protein Structures. J. Comp. Chem. 25:265–284, 2004.

62. Archontis, G. and Simonson, T. A residue-pairwise generalized born scheme suitable for protein design calculations. The journal of physical chemistry. B 109(47):22667–22673, December, 2005.

63. Grant, J. A., Pickup, B. T., Sykes, M. J., Kitchen, C. A., and Nicholls, A. The gaussian generalized born model: application to small molecules. Phys. Chem. Chem. Phys. 9(35):4913–4922, 2007.

64. Haberthür, U. and Caflisch, A. Facts: Fast analytical continuum treatment of solvation. J Comput Chem 29:701–715, October, 2007.

65. Srinivasan, J., Trevathan, M., Beroza, P., and Case, D. Application of a pairwise generalized Born model to proteins and nucleic acids: Inclusion of salt effects. Theor. Chem. Accts 101:426–434, 1999.

66. Wagoner, J. A. and Baker, N. A. Assessing implicit models for nonpolar mean solvation forces: the importance of dispersion and volume terms. Proc Natl Acad Sci U S A 103(22):8331–8336, May, 2006.

67. Spassov, V. Z., Yan, L., and Szalma, S. Introducing an implicit membrane in generalized born/solvent accessibility continuum solvent models. J. Phys. Chem. B 106(34):8726–8738, August, 2002.

68. Ulmschneider, M. B., Ulmschneider, J. P., Sansom, M. S., and Di Nola, A. A generalized Born implicit-membrane representation compared to experimental insertion free energies. Biophys J 92(7):2338–2349, April, 2007.

69. Tanizaki, S. and Feig, M. A generalized Born formalism for heterogeneous dielectric environments: application to the implicit modeling of biological membranes. The Journal of chemical physics 122(12), March, 2005.

70. Brooks, B., Bruccoleri, R., Olafson, D., States, D., Swaminathan, S., and Karplus, M. Charmm: A program for macromolecular energy, minimization, and dynamics calculations. Journal of Computational Chemistry 4:187–217, 1983.

71. MacKerel Jr., A., Brooks III, C., Nilsson, L., Roux, B., Won, Y., and Karplus, M. CHARMM: The Energy Function and Its Parameterization with an Overview of the Program, volume 1 of *The Encyclopedia of Computational Chemistry*, 271–277. John Wiley & Sons: Chichester, 1998.

72. Im, W., Feig, M., and Brooks, C. L. An implicit membrane generalized born theory for the study of structure, stability, and interactions of membrane proteins. Biophysical journal 85(5):2900–2918, November, 2003.

73. Simmerling, C., Strockbine, B., and Roitberg, A. E. All-Atom Structure Prediction and Folding Simulations of a Stable Protein. J. Am. Chem. Soc. 124:11258–11259, 2002.

74. Chen, J., Im, W., and Brooks, C. L. Balancing solvation and intramolecular interactions: toward a consistent generalized Born force field. J Am Chem Soc 128(11):3728–3736, March, 2006.

75. Jang, S., Kim, E., and Pak, Y. All-atom level direct folding simulation of a $\beta\beta\alpha$ miniprotein. The Journal of Chemical Physics 128(10):105102, 2008.

76. Zagrovic, B., Snow, C. D., Shirts, M. R., and Pande, V. S. Simulation of folding of a small alpha-helical protein in atomistic detail using worldwide-distributed computing. Journal of Molecular Biology 323(5):927–937, November, 2002.

77. Jang, S., Kim, E., Shin, S., and Pak, Y. Ab initio folding of helix bundle proteins using molecular dynamics simulations. J. Am. Chem. Soc. 125(48):14841–14846, December, 2003.

78. Lei, H. and Duan, Y. Ab initio folding of albumin binding domain from all-atom molecular dynamics simulation. J. Phys. Chem. B 111(19):5458–5463, May, 2007.

79. Pitera, J. W. and Swope, W. Understanding folding and design: replica-exchange simulations of "trp-cage" miniproteins. Proc Natl Acad Sci U S A 100(13):7587–7592, June, 2003.

80. Jagielska, A. and Scheraga, H. A. Influence of temperature, friction, and random forces on folding of the b-domain of staphylococcal protein a: All-atom molecular dynamics in implicit solvent. Journal of Computational Chemistry 28(6):1068–1082, 2007.

81. Lopes, A., Alexandrov, A., Bathelt, C., Archontis, G., and Simonson, T. Computational sidechain placement and protein mutagenesis with implicit solvent models. Proteins 67(4):853–867, June, 2007.

82. Felts, A. K., Gallicchio, E., Chekmarev, D., Paris, K. A., Friesner, R. A., and Levy, R. M. Prediction of protein loop conformations using the AGBNP implicit solvent model and torsion angle sampling. J. Chem. Theory Comput. 4(5):855–868, May, 2008.

83. Hornak, V., Okur, A., Rizzo, R. C., and Simmerling, C. HIV-1 protease flaps spontaneously open and reclose in molecular dynamics simulations. Proc Natl Acad Sci U S A 103(4):915–920, Jan, 2006.

84. Amaro, R. E., Cheng, X., Ivanov, I., Xu, D., and Mccammon, A. J. Characterizing loop dynamics and ligand recognition in human- and avian-type influenza neuraminidases via generalized born molecular dynamics and end-point free energy calculations. Journal of the American Chemical Society 131(13):4702–4709, 2009.

85. Tsui, V. and Case, D. Theory and Applications of the Generalized Born Solvation Model in Macromolecular Simulations. Biopolymers 56:275–291, 2001.

86. Sorin, E., Rhee, Y., Nakatani, B., and Pande, V. Insights into nucleic acid conformational dynamics from massively parallel stochastic simulations. Biophys J 85(2):790–803, Aug, 2003.

87. De Castro, L. F. and Zacharias, M. DAPI binding to the DNA minor groove: a continuum solvent analysis. J Mol Recognit 15(4):209–220, Jul-Aug, 2002.

88. Allawi, H., Kaiser, M., Onufriev, A., Ma, W., Brogaard, A., Case, D., Neri, B., and Lyamichev, V. Modeling of flap endonuclease interactions with DNA substrate. J. Mol. Biol. 328:537–554, 2003.

89. Chocholousová, J. and Feig, M. Implicit solvent simulations of DNA and DNA-protein complexes: agreement with explicit solvent vs experiment. J. Phys. Chem. B 110(34):17240–17251, Aug, 2006.

90. Ruscio, J. Z. and Onufriev, A. A computational study of nucleosomal DNA flexibility. Biophys J 91(11):4121–4132, Dec, 2006.

91. Spassov, V. Z., Yan, L., and Szalma, S. Introducing an implicit membrane in generalized Born/solvent accessibility continuum solvent models. J. Phys. Chem. B 106:8726–8738, 2002.

92. Zheng, W., Spassov, V., Yan, L., Flook, P., and Szalma, S. A hidden Markov model with molecular mechanics energy-scoring function for transmembrane helix prediction. Computational Biology and Chemistry 28(4):265–274, October, 2004.

93. Tanizaki, S. and Feig, M. Molecular dynamics simulations of large integral membrane proteins with an implicit membrane model. J Phys Chem B Condens Matter Mater Surf Interfaces Biophys 110(1):548–556, January, 2006.

94. Beroza, P. and Fredkin, D. R. Calculation of Amino Acid pK_{a}s in a Protein from a Continuum Electrostatic Model: Methods and Sensitivity Analysis. J. Comp. Chem. 17:1229–1244, 1996.

95. Antosiewicz, J., McCammon, J. A., and Gilson, M. K. Prediction of pH-dependent Properties of Proteins. J. Mol. Biol. 238:415–436, 1994.

96. Nielson, J. E. and Vriend, G. Optimizing the hydrogen-bond network in Poisson-Boltzmann equation-based pK_a calculations. Proteins 43:403–412, 2001.

97. Georgescu, R., Alexov, E., and Gunner, M. Combining conformational flexibility and continuum electrostatics for calculating pK$_a$s in proteins. Biophysical Journal 83:1731–1748, 2002.

98. Spassov, V. and Yan, L. A fast and accurate computational approach to protein ionization. Prot. Sci. 17:1955–1970, 2008.

99. Khandogin, J. and Brooks, C. L. Toward the accurate first-principles prediction of ionization equilibria in proteins. Biochemistry 45(31):9363–9373, August, 2006.

100. Ripoll, D. R., Vorobjev, Y. N., Liwo, A., Vila, J. A., and Scheraga, H. A. Coupling Between Folding and Ionization Equilibria: Effects of pH on the Conformational Preferences of Polypeptides. J. Mol. Biol. 264:770–783, 1996.

101. Lee, M. S., Salsbury, F. R., and Brooks, C. L. Constant-pH molecular dynamics using continuous titration coordinates. Proteins 56(4):738–752, Sep, 2004.

102. Khandogin, J. and Brooks, C. L. Linking folding with aggregation in alzheimer's beta-amyloid peptides. Proceedings of the National Academy of Sciences 104(43):16880–16885, October, 2007.

103. Mongan, J., Case, D. A., and McCammon, J. A. Constant pH molecular dynamics in generalized Born implicit solvent. J Comput Chem 25(16):2038–2048, Dec, 2004.

104. Swails, J. M., Meng, Y., Walker, A. F., Marti, M. A., Estrin, D. A., and Roitberg, A. E. ph-dependent mechanism of nitric oxide release in nitrophorins 2 and 4. The Journal of Physical Chemistry B 113(4):1192–1201, January, 2009.

105. Gohlke, H. and Case, D. A. Converging free energy estimates: MM-PB(GB)SA studies on the protein-protein complex ras-raf. J Comput Chem 25(2):238–250, January, 2004.

106. Liu, H. Y. and Zou, X. Electrostatics of ligand binding: Parametrization of the generalized Born model and comparison with the Poisson-Boltzmann approach. J. Phys. Chem. B 110(18):9304–9313, May, 2006.

107. Wittayanarakul, K., Hannongbua, S., and Feig, M. Accurate prediction of protonation state as a prerequisite for reliable MM-PB(GB)SA binding free energy calculations of HIV-1 protease inhibitors. Journal of Computational Chemistry 29(5):673–685, 2008.

108. Zou, X., Yaxiong, S., and Kuntz, I. D. Inclusion of solvation in ligand binding free energy calculations using the generalized-born model. J. Am. Chem. Soc. 121(35):8033–8043, September, 1999.

109. Ewing, T. J. A., Makino, S., Skillman, A. G., and Kuntz, I. D. Dock 4.0: Search strategies for automated molecular docking of flexible molecule databases. Journal of Computer-Aided Molecular Design 15:411–428, May, 2001.

110. Lee, M. S., Salsbury, F. R., and Olson, M. A. An efficient hybrid explicit/implicit solvent method for biomolecular simulations. J Comput Chem 25(16):1967–1978, Dec, 2004.

111. Okur, A., Wickstrom, L., Layten, M., Geney, R., Song, K., Hornak, V., and Simmerling, C. Improved efficiency of replica exchange simulations through use of a hybrid explicit/implicit solvation model. J. Chem. Theory Comput 2(2):420–433, 2006.

112. Okur, A. and Simmerling, C. Hybrid explicit/implicit solvation methods. In *Annual Reports in Computational Chemistry*, volume 2, 97–109. Elsiver, 2006.

113. Pellegrini, E. and Field, M. J. A generalized-born solvation model for macromolecular hybrid-potential calculations. J. Phys. Chem. A 106(7):1316–1326, February, 2002.

114. Walker, R. C., Crowley, M. F., and Case, D. A. The implementation of a fast and accurate qm/mm potential method in amber. Journal of Computational Chemistry 29(7):1019–1031, 2007.

115. Bashford, D. An object-oriented programming suite for electrostatic effects in biological molecules. In *Scientific Computing in Object-Oriented Parallel Environments*, Ishikawa, Y., Oldehoeft, R. R., Reynders, J. V. W., and Tholburn, M., editors, volume 1343 of *Lecture Notes in Computer Science*, 233–240 (ISCOPE97Springer, Berlin, 1997).

116. Friedrichs, M. S., Eastman, P., Vaidyanathan, V., Houston, M., Legrand, S., Beberg, A. L., Ensign, D. L., Bruns, C. M., and Pande, V. S. Accelerating molecular dynamic simulation on graphics processing units. Journal of Computational Chemistry 30(6):864–872, 2009.

117. Loncharich, R. J. and Brooks, B. R. The effects of truncating long-range forces on protein dynamics. Proteins 6:32–45, 1989.

118. Svrcek-Seiler, A. and Onufriev, A. Fast computation of effective Born radii for use in molecular dynamics simulations. in preparation.

119. Anandakrishnan, R. and Onufriev, A. V. An N log N approximation based on the natural organization of biomolecules for speeding up the computation of long range interactions. J. Comp. Chem. 31(4):691–706, 2010.

120. Hamelberg, D., Shen, T., and McCammon, J. A. Insight into the role of hydration on protein dynamics. The Journal of chemical physics 125(9), September, 2006.

121. Feig, M. Kinetics from implicit solvent simulations of biomolecules as a function of viscosity. J. Chem. Theory Comput. 3(5):1734–1748, September, 2007.

122. Hagen, S. J., Qiu, L., and Pabit, S. A. Diffusional limits to the speed of protein folding: fact or friction? Journal of Physics: Condensed Matter 17(18):S1503–S1514, 2005.

123. Lankas, F., Lavery, R., and Maddocks, J. H. Kinking occurs during molecular dynamics simulations of small dna minicircles. Structure 14(10):1527–1534, Oct, 2006.

124. Gordon, J. C., Fenley, A. T., and Onufriev, A. An analytical approach to computing biomolecular electrostatic potential. ii. validation and applications. The Journal of Chemical Physics 129(7):075102, 2008.

125. Shell, S. M., Ritterson, R., and Dill, K. A. A test on peptide stability of amber force fields with implicit solvation. J. Phys. Chem. B 112:6878–6886, May, 2008.

126. Zhou, R. and Berne, B. J. Can a continuum solvent model reproduce the free energy landscape of a beta -hairpin folding in water? Proc Natl Acad Sci U S A 99(20):12777–12782, Oct, 2002.

127. Roe, D. R., Okur, A., Wickstrom, L., Hornak, V., and Simmerling, C. Secondary structure bias in generalized born solvent models: Comparison of conformational ensembles and free energy of solvent polarization from explicit and implicit solvation. J. Phys. Chem. B 111(7):1846–1857, February, 2007.